THE JOURNAL OF BIOLOGICAL CHEMISTRY VOL. 287, NO. 13, pp. 10509–10524, March 23, 2012

Hypermethylated in Cancer 1 (HIC1) Recruits Polycomb Repressive Complex 2 (PRC2) to a Subset of Its Target Genes through Interaction with Human Polycomb-like (hPCL) Proteins*[S]

Received for publication, November 3, 2011, and in revised form, January 31, 2012 Published, JBC Papers in Press, February 7, 2012, DOI 10.1074/jbc.M111.320234

Gaylor Boulay[‡1], Marion Dubuissez[‡], Capucine Van Rechem[‡2], Antoine Forget[§3], Kristian Helin[¶], Olivier Ayrault[§3], and Dominique Leprince[‡4]

From the [‡]CNRS UMR 8161, Institut de Biologie de Lille, Université Lille Nord de France, Institut Pasteur de Lille, Lille 59021, France, the [§]Institut Curie, CNRS UMR 3306, INSERM U1005, Centre Universitaire, Orsay 91405, France, and the [¶]BRIC, University of Copenhagen, Ole Maaløes vej, 5, Dk-2200, Copenhagen, Denmark

Background: HIC1 is a transcriptional repressor recruiting CtBP and NuRD complexes.
Results: HIC1 interacts with human Polycomb-like proteins.
Conclusion: HIC1 recruits the *Polycomb* PRC2 on a subset of its target genes through interactions with Polycomb-like proteins.
Significance: Our results implicate hPCL proteins in the recruitment of PRC2 by transcription factors in mammals.

***HIC1* (*hypermethylated in cancer 1*) is a tumor suppressor gene epigenetically silenced or deleted in many human cancers. HIC1 is involved in regulatory loops modulating p53- and E2F1-dependent cell survival, growth control, and stress responses. *HIC1* is also essential for normal development because *Hic1*-deficient mice die perinatally and exhibit gross developmental defects throughout the second half of development. *HIC1* encodes a transcriptional repressor with five C_2H_2 zinc fingers mediating sequence-specific DNA binding and two repression domains: an N-terminal BTB/POZ domain and a central region recruiting CtBP and NuRD complexes. By yeast two-hybrid screening, we identified the *Polycomb-like* protein hPCL3 as a novel co-repressor for HIC1. Using multiple biochemical strategies, we demonstrated that HIC1 interacts with hPCL3 and its paralog PHF1 to form a stable complex with the PRC2 members EZH2, EED, and Suz12. Confirming the implication of HIC1 in *Polycomb* recruitment, we showed that HIC1 shares some of its target genes with PRC2, including *ATOH1*. Depletion of HIC1 by siRNA interference leads to a partial displacement of EZH2 from the *ATOH1* promoter. Furthermore, *in vivo*, *ATOH1* repression by HIC1 is associated with Polycomb activity during mouse cerebellar development. Thus, our results identify HIC1 as the first transcription factor in mammals able to recruit PRC2 to some target promoters through its interaction with *Polycomb-like* proteins.**

Polycomb are maintenance repressive complexes important for development, stem cell renewal, and cancer (1). Polycomb group (PcG)[5] proteins were first discovered in *Drosophila* for their role in the regulation of *Hox* genes during development and are now recognized as global epigenetic transcriptional regulators of cell fate decisions in all metazoans. They are organized in multiprotein modifying-chromatin complexes of variable composition (2). In mammals, the best characterized complexes are Polycomb repressive complexes 1 and 2 (PRC1 and PRC2). The PRC2 complex is composed of three core proteins, the histone methyltransferase EZH1 or EZH2, SUZ12, and one of the EED isoforms. EZH2 catalyzes the dimethylation and trimethylation of lysine 27 of histone 3 thereby generating an epigenetic repressive mark bound by the Polycomb (Pc) protein of PRC1 (2, 3).

In addition to these core components, PRC2 is associated with co-factors that are essential to modulate its activity and/or its recruitment to specific loci in embryonic stem cells, such as the recently characterized JARID2 protein, which contains an AT-rich DNA-binding domain (4, 5). However, the first PRC2 co-factor, Polycomb-like (PCL) was discovered in *Drosophila* through biochemical characterization of a 1-MDa complex distinct from the prominent 600-kDa E(z) complex PRC2 (6). In line with the significant expansion of *PcG* genes during evolution, three human orthologs of *Drosophila Polycomb-like* have been characterized, *hPCL1/PHF1* (*human Polycomb-like 1/PHD finger protein 1*) (7), *hPCL2/MTF2* (7, 8), and *hPCL3/PHF19* (9). These three genes are differentially expressed suggesting that their expression pattern could provide other potential regulatory mechanisms to PcG target genes. Indeed, *PHF1* and *hPCL3* are widely expressed in different normal tissues with some examples of co-expression (7, 8). *hPCL3* is also

* This work was supported in part by grants from the CNRS, the Ligue Nationale contre le Cancer (Comité Interrégional du Septentrion), the Fondation pour la Recherche Médicale (Comité du Nord), and the Association pour la Recherche contre le Cancer (to D. L.).
[S] This article contains supplemental Fig. S1 and Table S1.
[1] Supported by fellowships from the CNRS/Région Nord-Pas de Calais and the Association pour la Recherche contre le Cancer.
[2] Present addresses: Harvard Medical School and Massachusetts General Hospital Cancer Center, Charlestown, MA 02129.
[3] Supported by a AVENIR/INSERM/Inca grant.
[4] To whom correspondence should be addressed: CNRS UMR8161, Institut de Biologie de Lille, 1 Rue du Professeur Calmette, BP 447, 59021 Lille Cedex, France. Tel.: 00-33-3-20-87-11-19; Fax: 00-33-3-20-87-11-11; E-mail: dominique.leprince@ibl.fr.

[5] The abbreviations used are: PcG, Polycomb group; PRC, Polycomb repressive complex; PCL, Polycomb-like; PHD, plant homeodomain; qRT, quantitative reverse transcriptase; CR, central region; NLS, nuclear localization signal. ESC, extra sex combs; EED, embryonic ectoderm development; Suz12, suppressor of zeste 12; EZH2, enhancer of zeste homolog 2.

up-regulated in many cancers (9). By contrast, microarray analyses in mice have demonstrated that *Pcl2* is highly expressed in undifferentiated embryonic stem cells and during embryonic development as well as in some adult tissues (8). PHF1, hPCL2, and hPCL3 are highly similar and display strong sequence similarities to *Drosophila* PCL. In particular, they share an N-terminal module consisting of three well defined functional domains, namely a TUDOR domain and two adjacent PHD (plant homeodomain) fingers immediately followed by a domain of extended homology with *Drosophila* PCL (8–10). These PCL proteins are not implicated in the formation and stability of the PRC2 complex in contrast with EED and SUZ12 but are essential for high levels of H3K27 trimethylation in *Drosophila* (11) and mammals (12, 13) as well as for the cell-specific targeting of PRC2 to specific loci such as some *Hox* genes (8, 14, 15).

HIC1 (*hypermethylated in cancer 1*) is a tumor suppressor gene frequently deleted or epigenetically silenced in many human cancers (16, 17). *HIC1* is a *bona fide* tumor suppressor because $Hic1^{+/-}$ heterozygous mice have a high propensity to spontaneously develop tumors late in life (18). In addition, HIC1 synergizes with P53 in tumor suppression (19). *HIC1* is a direct target of P53 and represses the transcription of *SIRT1*, a NAD^+-dependent class III deacetylase that deacetylates and inactivates P53, thereby modulating P53-dependent DNA damage responses (20). Similarly, SIRT1 and HIC1 are also involved in a feedback regulatory loop with E2F1, a crucial activator of SIRT1 transcription in response to DNA damage. E2F1 activates *HIC1* (21) and is inactivated by SIRT1-mediated deacetylation (22). Thus, HIC1 is placed at the crossroads of complex regulatory loops modulating P53-dependent and E2F1-dependent cell survival, growth control, and stress responses (17, 23). In addition, *HIC1* is also essential for normal mammalian development as shown by $Hic1^{-/-}$ homozygous mice, which together with a perinatal death have several developmental anomalies resembling those found in Miller-Dieker syndrome patients (24, 25).

HIC1 encodes a sequence-specific transcriptional repressor with five Krüppel-like C2H2 zinc fingers and two autonomous repression domains: the N-terminal BTB/POZ domain and its central region (16, 17, 26). To date, only 12 direct target genes supporting roles in development, cell cycle, and cell migration regulation have been described for HIC1 (reviewed in Refs. 27–30). HIC1 recruits different co-repressor complexes to its target genes through conserved small peptide motifs located in its central region, such as CtBP complexes through a GLDLSKK motif (31). In addition a SUMOylation/acetylation switch on lysine 314 embedded in the $\psi K^{314}XEP$ motif in the HIC1 central region regulates recruitment of the NuRD complex. Indeed, the interaction with MTA1, a component of the NuRD complex is regulated by these two competitive post-transcriptional modifications at lysine 314, promotion by SUMOylation, and inhibition by acetylation (27). So far, few HIC1 target genes are known and its mechanisms of transcriptional repression are still poorly understood.

In this study, by yeast two-hybrid screening with the two repression domains of HIC1 as bait (BTB-CR-LexA), we identified hPCL3 as a novel corepressor for HIC1. We show that HIC1 interacts with the two hPCL3 isoforms, hPCL3L and hPCL3S, as well as with the related PHF1 paralog. HIC1 recruits PRC2 independently of the CtBP and NuRD complexes, which interact with the HIC1 central region, and we further demonstrate that this interaction mainly relies on its BTB/POZ domain. On the other hand, the common TUDOR domain and the hPCL3L-specific PHD2 domain are both involved in the interaction with HIC1. However, although both hPCL3L and hPCL3S isoforms interact with HIC1 and EZH2, only hPCL3L favors the formation of a ternary complex with HIC1 and PRC2 components. Consistent with these findings, we demonstrate that, in normal WI38 fibroblasts, HIC1 recruits PHF1 and the PRC2 complex to some HIC1 target genes such as *ATOH1* as well as the *EFNA1* and *CXCR7* promoters, as shown by the detection of high levels of H3K27 trimethylation and EZH2. Functional analyses using RNAi knockdown demonstrate that HIC1 is necessary for the stable recruitment of EZH2 on *ATOH1* in WI38 and BJ-tert cells. Finally, *in vivo* during mouse cerebellar development, *ATOH1* repression by HIC1 is associated with Polycomb-mediated epigenetic activity. In conclusion, our results identify HIC1 as the first transcription factor in mammals able to recruit the repressive PRC2 complex to a discrete subset of target genes through its interaction with *Polycomb-like* proteins.

EXPERIMENTAL PROCEDURES

Yeast Two-hybrid Screen—Yeast two-hybrid screening was performed by Hybrigenics, Paris, France, as previously described (32). For bait cloning, the BTB-Central Region of HIC1(1–422) encompassing the two autonomous repression domains was PCR amplified and cloned in-frame with a C-terminal LexA DNA-binding domain in a yeast two-hybrid vector. A human breast tissue random-primed cDNA library, transformed into the Y187 yeast strain and containing 10 million independent fragments, was used for mating. The screen was performed in conditions ensuring a minimum of 50 million interactions tested, to cover five times the primary complexity of the yeast-transformed cDNA library. 79 million interactions were actually tested with HIC1.

Cell Culture—WI-38 were purchased from ATCC (14 passages) and cultured in minimal essential medium (Invitrogen) supplemented with 10% fetal calf serum (FCS), nonessential amino acids,and gentamicin. HEK293T cells were maintained in DMEM (Invitrogen) supplemented with 10% FCS, gentamicin, and nonessential amino acids. BJ-tert cells were maintained in DMEM supplemented with 10% FCS and penicillin/streptomycin.

Plasmids and shRNA Retroviral Infections—The pTL1-HIC1, pcDNA3-FLAG-HIC1, pcDNA3-FLAG-HIC1 L225A, K314R, E316A, and K314Q expression vectors as well as BTB-Gal4-NLS-HA and BTB-CR-Gal4-NLS-HA HIC1 chimeras have been previously described (31, 33). The expression vectors for full-length FLAG-hPCL3L and FLAG-hPCL3S or for their isolated domains (10), as well as for Myc-EZH2 (34), HA-EED, and HA-SUZ12 (35, 36) have been previously described.

We PCR amplified and cloned a fragment corresponding to full-length PHF1 and amino acids 2–240 (containing the TUDOR and the two tandem PHD domains) of PHF1 flanked

by BamHI and EcoRI restriction sites into pcDNA3-FLAG. All constructs were verified by sequencing. shRNA were cloned in the pSuperRetro vector according to the manufacturer's instructions using previously published sequences targeting PHF1 (12) and HIC1 (37). BJ-tert cells were infected with retrovirus encoding shRNA as previously described (30) for 24 h, fresh medium was added for 24 h and infected cells were selected for 48 h by puromycin treatment at 2 μg/ml.

Antibodies—Rabbit polyclonal anti-HIC1 (325 and 2563) antibodies (31), the monoclonal antibodies against EZH2 (AC22), EED (AA19), and Bmi1 (AF27) (35, 36), and the polyclonal antibodies against the C-terminal end of hPCL3L (10) have been previously described. For HIC1 immunoblotting shown in Figs. 1*E*, 8*E*, 9*A*, and 10*A*, we used a new batch of polyclonal antibodies obtained by injecting a synthesized peptide corresponding to the C-terminal end of HIC1 into New Zealand rabbits (Eurogentec, Seraing, Belgium). Similarly, to generate polyclonal antibodies against PHF1, two peptides were synthesized and used to immunize two New Zealand rabbits. Their sequences are (amino acids 360–374) H2N-CGV SRP LGK RRR PEP E-CONH2 and (amino acids 312–327) H2N-HKD RFI SGR EIK KRK C-CONH2. Commercial antibodies of the following specificity were used: FLAG from Sigma (M2 monoclonal antibody F3165); GAL4 (sc-577), ACTIN (sc-1616-R), GAPDH (sc-32233), and MYC tag (sc-789) were from Santa Cruz; HA (mouse monoclonal from BABCO); anti-Suz12 ((D39F6) from Cell Signaling; anti-H3K27me3 (07-449) and anti-acetyl Histone H3 (06-599) from Upstate; anti-H3K27me2 (39245) from Active motif; anti-Histone H3 (ab1791) from Abcam.

Transfection and Co-immunoprecipitation Assays—Cells were transfected in Opti-MEM (Invitrogen) by the polyethyleneimine method using ExGen 500 (Euromedex), as previously described (10). Cells were transfected for 6 h and then incubated in fresh complete medium. For co-immunoprecipitation assays, 48 h after transfection, cells were rinsed twice in ice-cold PBS and lysed in ice-cold IPH buffer (50 mM Tris/HCl, pH 8, 150 mM NaCl, 5 mM EDTA, 0.5% Nonidet P-40, and 1× protease inhibitor mixture (Roche Applied Science)). Cell lysates were cleared by centrifugation (20,000 × *g*, at 4 °C for 30 min). The supernatants were incubated overnight at 4 °C with 2 μg of antibody. Then, protein A/G-Sepharose beads (Amersham Biosciences) were added for 30 min. The beads were washed 3 times with IPH buffer. Proteins were eluted by boiling in Laemmli loading buffer and separated by SDS-PAGE (8, 12, or 15%) before Western blotting.

Sequential co-immunoprecipitation were performed essentially as described above. Briefly, after a first round of immunoprecipitation with FLAG antibodies coupled to agarose beads (Sigma), FLAG-HIC1 and associated proteins were eluted with 100 μl of a FLAG peptide/TBS (50 mM Tris/HCl, 150 mM NaCl, pH 7.4) solution according to the manufacturer's instructions. 900 μl of IPH buffer were then added and subjected to a second immunoprecipitation with anti-hPCL3L antibody. Co-immunoprecipitation analyses of endogenous proteins associated with chromatin in normal WI-38 fibroblasts and HEK293T transiently transfected with FLAG-HIC1 were performed as previously described (10) or as described above, except that the lysates were extensively sonicated before the clearing centrifugation step.

Western Blot—Western blots were performed as previously described (10, 31). The secondary antibodies were horseradish peroxidase-linked antibodies raised against rabbit or mouse immunoglobulins (Amersham Biosciences).

Small Interfering RNAs—WI-38 cells were reverse-transfected with RNAiMax (Invitrogen) according to the manufacturer's instructions using 20 nM small interfering RNA targeting *HIC1* (HIC1 siGENOME Smart Pool M-006532-01, Dharmacon), *EZH2* (siGENOME Smart Pool M-004218-03), or a scrambled sequence. 72 h later cells were harvested for protein, RNA, or chromatin extraction. In Fig. 10, cells were incubated for 6 days using 5 nM small interfering RNA.

Chromatin Immunoprecipitation—Conventional ChIP and sequential ChIP were performed as previously described (10). The purified DNAs were used for PCR analyses with Fast Start TaqDNA Polymerase (Roche Applied Science) using the relevant primers for *ATOH1* and *GAPDH* (supplemental Table S1).

Quantitative ChIP was performed according to the Q^2 ChIP protocol as previously described with slight modifications (38). Briefly, formaldehyde was added directly to the cultured cells to a final concentration of 1% for 15 min at 37 °C. Adding glycine to a final concentration of 0.125 M stopped the cross-linking. After 5 min at 37 °C, cells were lysed directly in the plates by resuspension in cell lysis buffer for 5 min. Then, the samples were pelleted, resuspended in nuclei lysis buffer, and sonicated to chromatins with an average size of 250 bp using a BioRuptor (Diagenode, Liege, Belgium). Whole postnatal day 5 (P5) mice cerebella (C57BL/6 background) were immersed in 1% formaldehyde in PBS for 2.5 h on ice, whereas P21 cerebella (C57BL/6 background) were first cut into 4 pieces. Glycine was added to 250 mM and incubated for 5 min at room temperature. After washing with PBS, samples were extensively resuspended in 500 μl of cell lysis buffer, incubated 10 min on a rotator at 4 °C, and centrifuged. Pellets were then resuspended in 200 μl of nuclei lysis buffer, separated into two tubes, and sonicated with 9 sets of 30-s pulses using a BioRuptor at the highest power. Chromatin was diluted to a concentration of 1.5 A_{260} units in RIPA buffer (10 mM Tris/HCl, pH 7.5, 1 mM EDTA, 0.5 mM EGTA, 1% Triton X-100, 0.1% SDS, 0.1% sodium deoxycholate, 140 mM NaCl). Chromatin (100 μl, 1.5 A_{260} units) was transferred to a tube containing 2.4 μg of antibody-magnetic protein A-coated bead (Millipore) complexes in 100 μl of RIPA buffer and incubated overnight on a rotator at 4 °C. Immune complexes were washed three times in ice-cold RIPA buffer and once in TE buffer (10 mM Tris/HCl, pH 8, 10 mM EDTA). Each wash lasted for 4 min on a rotator at room temperature. ChIP complexes were transferred to a new tube with TE buffer, which was removed and replaced by 150 μl of elution buffer (20 mM Tris/HCl, pH 7.5, 50 mM NaCl, 1% SDS) containing 50 μg/ml of proteinase K and incubated 1 h at 55 °C. Then samples were treated with 133 μg/ml of RNase A for 30 min at 37 °C. Finally, the supernatant was recovered and incubated for 2 h at 68 °C. DNAs as well as 5% input (5 μl of 1.5 A_{260} units) were purified on Nucleobond Extract II (Macherey-Nagel) and eluted with 150 μl of H_2O. The protocol involving mouse use was per-

formed in accordance with the National and European regulation on the protection of animals used for scientific purposes.

RT-PCR and Quantitative PCR—RNA extraction, reverse transcription, and quantitative PCR were performed as previously described (10).

Immunoprecipitated DNA was analyzed in a MX3005P fluorescence temperature cycler (Stratagene) in triplicates by real time PCR starting from 3 μl of template DNA in a final volume of 10 μl containing power SYBR Green (Applied Biosystems) and primers at a final concentration of 0.5 μM. The primers used are summarized in supplemental Table S1. According to a melting point analysis, only one PCR product was amplified under these conditions. An input control was used to generate a standard curve for each gene. Results were expressed as % input for EZH2 and as a ratio of total histone H3 for acetyl-H3, H3K27me3, and H3K27me2. Each condition was performed twice and a representative experiment is shown.

Statistics—Experiments were performed at least twice independently in duplicates or triplicates. Statistical analyses were performed by Student's *t test*. The asterisk (*) indicates $p < 0.05$.

RESULTS

HIC1 Interacts with hPCL3L and PHF1—To further characterize the repression mechanisms brought about by HIC1 on its target genes, we conducted a yeast two-hybrid screen using the two autonomous repression domains of HIC1, the BTB/POZ domain and the central region, as bait to screen a human mammary gland library (Fig. 1*A*). As previously described, this screen has already identified in addition to CtBP, ARID1A/BAF250A, a component of the SWI/SNF complexes and MTA1, a component of the NuRD repressive complexes as new HIC1 partners (27, 32). In addition, seven interacting clones corresponded to the N-terminal half (amino acids 32–361) of hPCL3 (human Polycomb-like 3), one of the three human orthologs of the *Drosophila* PCL (Polycomb-like) protein (9). The isolated preys contained the TUDOR domain, the two plant homeodomain (PHD) fingers, and the domain of extended homology with *Drosophila* PCL demonstrating that they corresponded to the longest isoform of hPCL3, hPCL3L (9, 10) (Fig. 1*A*). Because hPCL3 is functionally linked to the PRC2 Polycomb repressive complexes (10), we decided to further study this potential new HIC1 interacting protein.

To confirm this interaction, we first performed coimmunoprecipitation analyses in transiently transfected HEK293T cells. HIC1 was coprecipitated by FLAG-hPCL3L (Fig. 1*B*) and conversely, FLAG-hPCL3L was coimmunoprecipitated by HIC1 (Fig. 1*C*) demonstrating that full-length HIC1 and hPCL3 associate *in vivo*. Furthermore, as shown in Fig. 6*B*, FLAG-HIC1 proteins can efficiently co-immunoprecipitate endogenous hPCL3L in HEK293T.

The *Drosophila* PCL has three human homologues, PHF1 (hPCL1), hPCL2, and hPCL3, which exhibit distinct expression patterns (8, 9). However, these three homologues are highly related notably for the presence of the TUDOR and tandem PHD domains. Previously, we demonstrated through quantitative RT-PCR analyses that PHF1 but not hPCL3 is highly expressed together with HIC1 in normal human WI38 fibroblasts (10). Because these WI-38 cells are a convenient model to study the functional properties of endogenous HIC1 proteins (20, 27), we asked whether HIC1 could also interact with PHF1. As expected from their common structural organization, HIC1 was coimmunoprecipitated by FLAG-PHF1 (Fig. 1*D*) and conversely FLAG-PHF1 was coprecipitated by HIC1 (Fig. 1*E*). According to our previous results of qRT-PCR in mammary HMEC-hTERT and MCF10A cells (10), PHF1 appeared less expressed than hPCL3L in the human mammary gland, the tissue used to construct the library for the yeast two-hybrid screen. This result could at least partly explain why PHF1 was not initially identified as a potential HIC1 partner. Thus, our results demonstrate that HIC1 interacts with two Polycomb-like proteins, hPCL3 and PHF1.

HIC1 Recruits hPCL3L via Its BTB/POZ Domain and Independently of CtBP and NuRD Complexes—The bait used in the two-hybrid screen included the two repression domains of HIC1, the BTB/POZ domain and the central region (CR) in-frame with a C-terminal DNA-binding domain to mimic the structure of the wild-type HIC1 protein. The CtBP and MTA1 corepressors isolated in this screen clearly interact with the central region, respectively, through the GLDLSKK motif and the MKHEP SUMOylation/acetylation switch motif (Fig. 1*A*) (27, 31, 33).

The CtBP and NuRD repression complexes have been linked, respectively, to the recruitment of PcG proteins and to the deposit of its specific epigenetic mark, H3K27me3 (39–41). To investigate a potential link in the case of HIC1, we performed co-immunoprecipitation analyses between hPCL3L and HIC1 point mutants compromised in their ability to interact with these two complexes. The HIC1 L225A mutant carries a point mutation in the GLDLS motif that abrogates its interaction with CtBP (42). Several point mutants in the SUMOylation/acetylation switch motif MK^{314}HEP severely impaired the interaction between HIC1 and MTA1, a component of the NuRD complex (27). The CtBP-deficient mutant displayed an ability to interact with hPCL3L comparable with its wild-type counterpart (Fig. 2*A*). Similarly, neither the SUMOylation-deficient mutants K314R and E316A nor the K314Q mutant mimicking a constitutive acetylation showed significantly reduced binding to hPCL3 compared with wild-type HIC1 (Fig. 2*B*).

We thus hypothesize that the BTB/POZ domain could be the HIC1 repression domain implicated in the interaction with hPCL3L. To that end, we used BTB- and BTB-CR-Gal4 chimeras including a nuclear localization signal (NLS) and an HA epitope, as previously described (33) (Fig. 3*A*). The isolated central region cannot be tested in this experimental setting due its conformational problems in the absence of the BTB/POZ domain (31). In transient transfection assays, the BTB-CR-Gal4 chimera interacts with hPCL3L in close agreement with the yeast two-hybrid screen (Fig. 3*B*, *lane 5*). Interestingly, a strong interaction was also detected with the isolated BTB/POZ domain (Fig. 3*B*, *lane 4*). In contrast with the related BTB/POZ domains of BCL6 and PLZF, the HIC1 BTB/POZ domain is an HDAC-independent repression domain insensitive to inhibitors of Class I and II HDACs such as TSA (43). Aside from the Class III deacetylase SIRT1 (20), hPCL3L is therefore only the second protein described so far as interacting with the HIC1 BTB/POZ domain. These observations indicate that HIC1 can

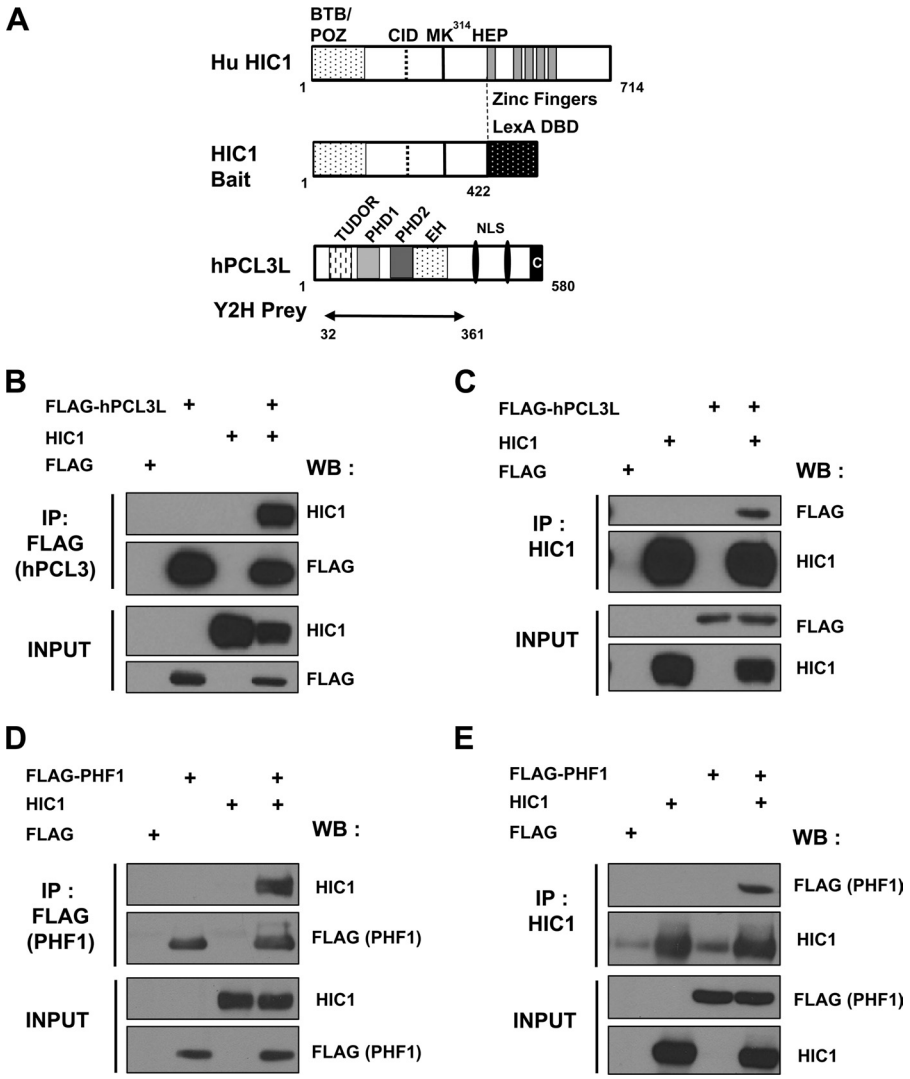

FIGURE 1. **HIC1 interacts with hPCL3 and its paralogue PHF1 (PHD finger protein 1).** *A,* schematic drawing of the human HIC1 and hPCL3L (human Polycomb-like 3) proteins. The BTB/POZ domain, the central region containing the evolutionarily conserved CtBP-interaction domain (*CID*) (31), the acetylation/SUMOylation switch motif (ψK^{314}XEP) (27, 33), and the 5 C_2H_2 zinc fingers are shown. The fragment of HIC1 used as the bait for two-hybrid screening of a human mammary gland cDNA library included the two autonomous repression domains of HIC1 (amino acids 1–422). The BTB/POZ domain and the central region were fused in-frame with a C-terminal LexA DNA-binding domain (*DBD*) to mimic the HIC1 protein. The longest isoform of human Polycomb-like 3 protein, hPCL3L (Q5T6S3: 580 amino acids), is shown *below*. The domains conserved within the human Polycomb-like family are *boxed*, including the conserved TUDOR, plant homeodomain (*PHD1*), and PHD2 domains, the PCL extended homology domain (*EH*) and a C-terminal Chromo-like domain (*C*) (9, 10). Two predicted NLS are shown as *black ovals*. The isolated prey corresponds to amino acids 32–361 of hPCL3L. *B*, HIC1 interacts with hPCL3L. HEK293T cells were transfected for 48 h with the indicated expression plasmids as well as with the empty pcDNA3-FLAG vector as control. Whole cells extracts were prepared in IPH buffer, incubated with anti-FLAG antibodies, and immunoblotted (*WB*). The relevant pieces of the membranes were incubated with polyclonal antibodies against HIC1 to detect co-immunoprecipitation (*IP*) or with anti-FLAG monoclonal antibodies to ascertain the presence of hPCL3L (*IP*: *FLAG*). 2% of each lysate were directly resolved by SDS-PAGE and immunoblotted with the indicated antibodies (*INPUT*). *C,* hPCL3L interacts with HIC1. The reciprocal experiment was performed in HEK293T cells with the same combinations of expression plasmids but using the polyclonal anti-HIC1 antibodies for the immunoprecipitation step. *D*, HIC1 interacts with PHF1. HEK293T cells were transiently transfected for 48 h with the indicated expression plasmids. Whole cells extracts were prepared in IPH buffer and incubated with anti-FLAG antibodies (*top panels*, IP FLAG (PHF1), *first to fourth lanes*) and immunoblotted (*WB*) with polyclonal antibodies against HIC1 to detect co-immunoprecipitation. The membrane was then stripped and re-probed with anti-FLAG monoclonal antibodies to ascertain the presence of PHF1. 2% of each lysate were directly resolved by SDS-PAGE and immunoblotted with the indicated antibodies (*bottom panels*: *INPUT*). *E*, PHF1 interacts with HIC1. The reciprocal experiment was performed in HEK293T cells with the same combinations of expression plasmids but using polyclonal anti-HIC1 antibodies for the immunoprecipitation step. Note that the new batch of antibodies used in this experiment is able to detect the weak amount of endogenous HIC1 proteins present in HEK293T after a first HIC1 immunoprecipitation.

recruit independently three distinct repression complexes through its BTB/POZ domain and central region.

The Two hPCL3 Isoforms Interact with HIC1 via Their TUDOR and PHD2 Domains—The full-length hPCL3L protein contains a TUDOR domain and two tandem zinc finger-like PHD domains, PHD1 and PHD2, which were all included in the isolated prey (Fig. 1*A*). The hPCL3 gene also encodes a shorter isoform, which contains only the TUDOR and PHD1 domains (Fig. 4*A*) (9). In transient transfection assays, HIC1 is co-immunoprecipitated by this shorter isoform (Fig. 4*B*). To determine which domain is responsible for the interaction with HIC1, we conducted co-immunoprecipitation assays between HIC1 and our previously described FLAG-tagged deletion mutants (Fig. 4*A*) (10). As shown in Fig. 4*C*, a strong interaction was detected between HIC1 and the N-terminal half of hPCL3S containing the TUDOR domain (*lane 3*) or with the isolated PHD2 domain

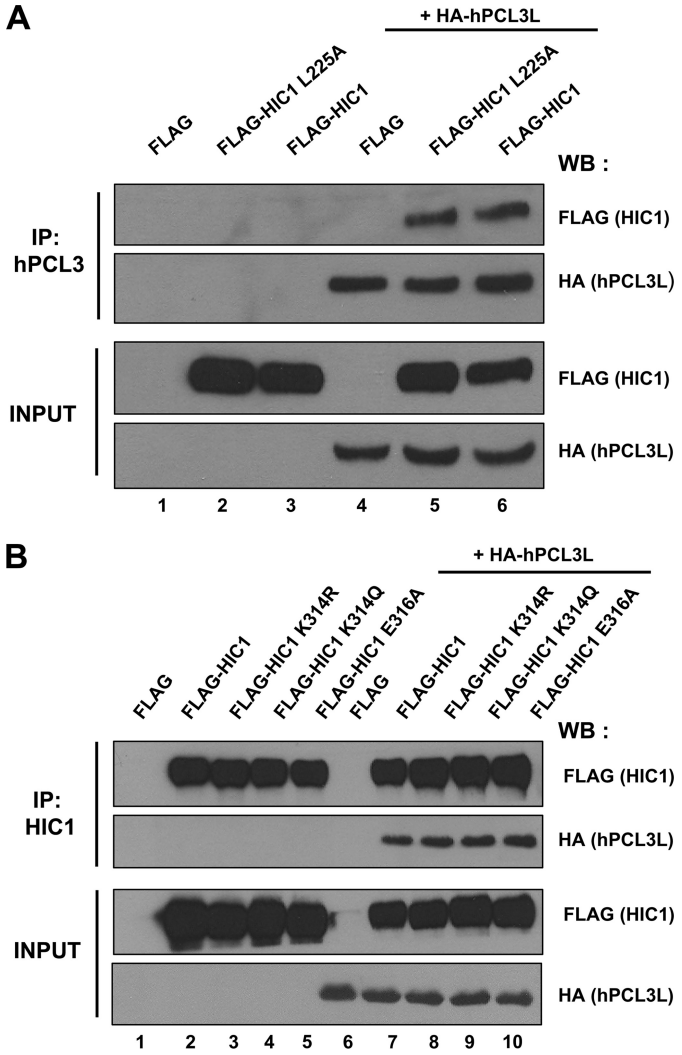

FIGURE 2. **HIC1 recruits hPCL3L independently of the CtBP and NuRD complexes.** *A*, the HIC1 L225A mutant that is unable to interact with CtBP recruits hPCL3 as efficiently than wtHIC1. HEK293T cells were transiently transfected with the indicated combination of FLAG- and HA-tagged versions of HIC1 and hPCL3L as well as with the empty pcDNA3-FLAG vector as a control. Whole cell extracts were prepared in IPH buffer and incubated with anti-hPCL3L antibodies (*IP*: hPCL3L, *lanes 1–6*) and immunoblotted (*WB*) with anti-FLAG antibodies to detect co-immunoprecipitation of HIC1 (*top panel*). The blot was then stripped and probed with anti-HA to verify the presence of hPCL3L in the relevant immunoprecipitates (*second panel*). 2% of each lysate was directly resolved by SDS-PAGE and successively immunoblotted with anti-FLAG and anti-HA antibodies (*INPUT*, *two bottom panels*, *lanes 1–6*). *B*, the acetylation/SUMOylation switch on lysine 314 does not regulate the interaction with hPCL3L. The various SUMOylation-deficient mutants K314R and E316A as well as the K314Q mutant mimicking a constitutive acetylation have been previously described (27). They were used together with the HA-hPCL3L and the empty pcDNA3-FLAG vector as control in a co-immunoprecipitation experiment as described above.

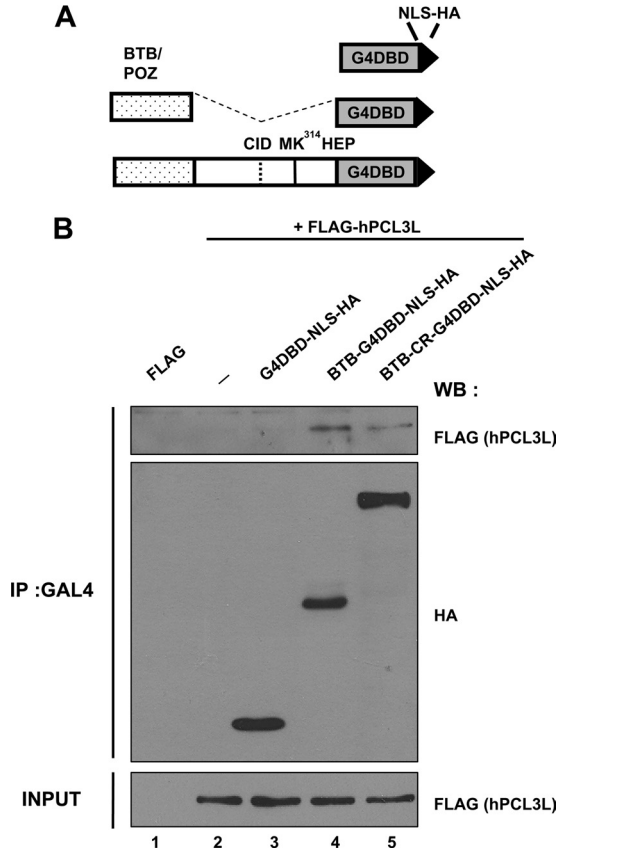

FIGURE 3. **The HIC1 BTB/POZ domain interacts with hPCL3L.** *A*, schematic representation of the various Gal4DBD-NLS-HA chimeras. *B*, association of hPCL3L with HIC1 is dependent on the BTB/POZ domain. HEK293T cells were transiently transfected with the indicated expression plasmids as well as with the empty Gal4DBD-NLS-HA vector as a control for 48 h. Whole cells extracts were prepared in IPH buffer and incubated with anti-GAL4 antibodies (*top panels*, IP GAL4, *lanes 1–5*) and immunoblotted (*WB*) with anti-HA monoclonal antibodies to verify the presence of the HIC1-Gal4 chimeras in the immunoprecipitates and with antibodies against the FLAG epitope to detect hPCL3L co-immunoprecipitation. 2% of each lysate was directly resolved by SDS-PAGE and immunoblotted with antibodies against FLAG to ascertain the presence of hPCL3L (*bottom panel*: *Input*, *lanes 1–5*).

(*lane 5*). By contrast, a very weak interaction was detected between HIC1 and the C-terminal half of hPCL3S containing the PHD1 domain (Fig. 4*C*, *lane 4*). Notably, the PHD1 domain is poorly conserved in the phylogeny of PCL3 proteins in striking contrast with the TUDOR and PHD2 domains (10). In accordance with a conserved mechanism of interaction between HIC1 and Polycomb-like proteins, a truncated form of PHF1 containing its TUDOR, PHD1, and PHD2 domains was sufficient to co-immunoprecipitate HIC1 (Fig. 4*D*).

In conclusion, these results demonstrate that both the TUDOR and PHD2 domains are required for the interaction with HIC1. Notably, these two domains interacting with HIC1 are also involved in the interaction with EZH2 (10).

hPCL3L Favors Formation of a Ternary Complex with HIC1 and PRC2 Complex—We finally decided to clarify the role of these interactions between HIC1 and Polycomb-like proteins. Although they contain different combinations of functional domains, the two hPCL3 isoforms interact both with HIC1 (Figs. 1*B* and 4*B*) and EZH2 and EED, two components of PRC2 complexes (10). Nevertheless, hPCL3L and hPCL3S display different subcellular localizations and are present in two different EZH2 containing complexes as previously shown by gel filtration analyses (10). These observations prompted us to investigate whether both hPCL3 isoforms could form a "ternary" complex with HIC1 and components of the PCR2 complex. In a preliminary experiment, the three components necessary to obtain a stable PRC2 complex, EZH2, EED, and SUZ12, were cotransfected together with HIC1 and with or without each of the two hPCL3 isoforms. HIC1 proteins were immunoprecipitated with FLAG antibodies and their associated proteins were

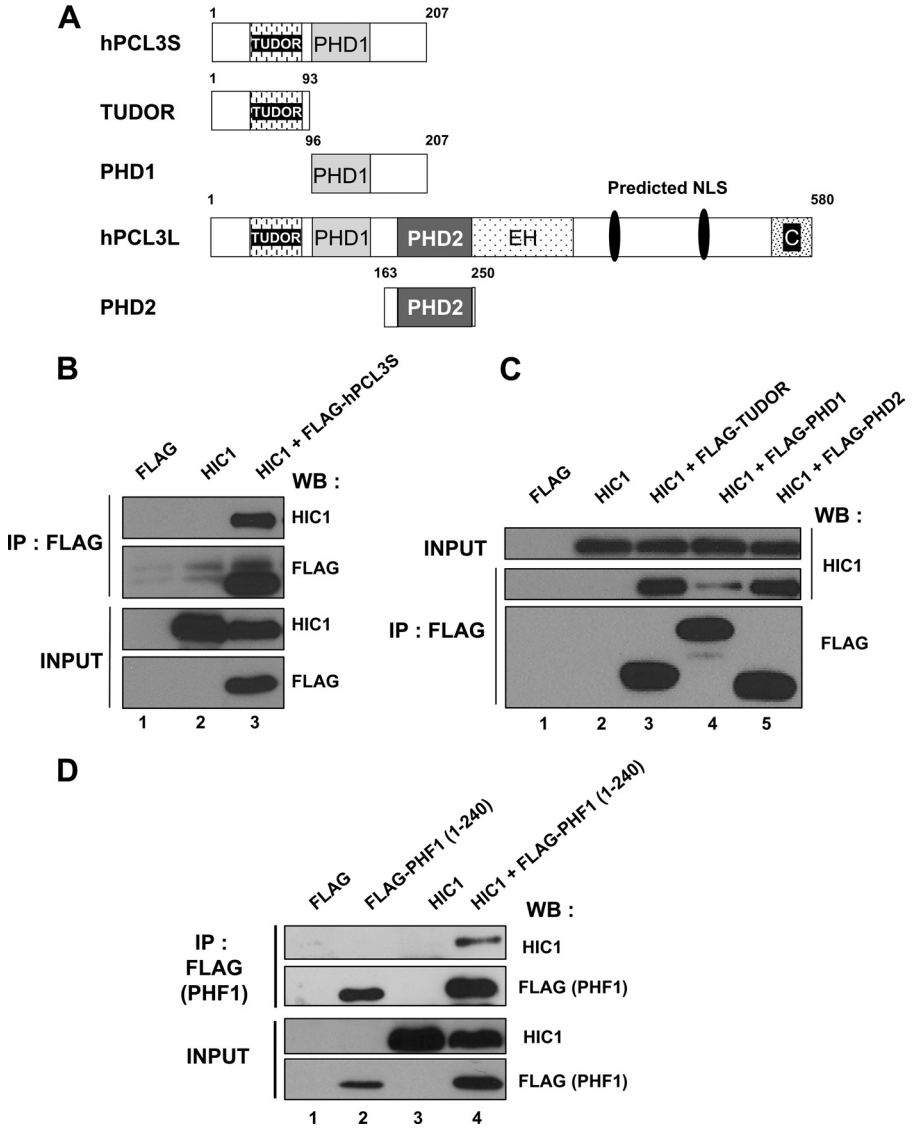

FIGURE 4. **HIC1 interacts with the two hPCL3 isoforms, hPCL3L and hPCL3S, via their conserved TUDOR and PHD2 domains.** *A*, schematic representation of the hPCL3L and hPCL3S isoforms and deletion mutants used. *B,* HIC1 also interacts with the hPCL3S isoform. HEK293T cells were transfected for 48 h with the indicated expression plasmids as well as with the empty pcDNA3-FLAG vector as control. Whole cells extracts were prepared in IPH buffer, incubated with anti-FLAG antibodies and immunoblotted (*WB*). The relevant pieces of the membranes were incubated with polyclonal antibodies against HIC1 to detect co-immunoprecipitation (*IP*) or with anti-FLAG monoclonal antibodies to ascertain the presence of hPCL3S (*IP: FLAG*). 2% of each lysate were directly resolved by SDS-PAGE and immunoblotted with the indicated antibodies (*INPUT*). *C,* association of HIC1 with hPCL3 is dependent on the TUDOR and PHD2 domains. HEK293T cells were transiently transfected with the indicated expression plasmids as well as with the empty pcDNA3-FLAG vector as a control for 48 h. Whole cells extracts were prepared in IPH buffer and incubated with anti-FLAG antibodies (*two bottom panels*: *IP FLAG*, *lanes 1–5*) and immunoblotted (*WB*) with anti-HIC1 antibodies to detect HIC1 co-immunoprecipitation (*middle panel*) and with anti-FLAG monoclonal antibodies to verify the presence of hPCL3 deletion mutants in the immunoprecipitates (*bottom panel*). 2% of each lysate was directly resolved by SDS-PAGE and immunoblotted with antibodies against HIC1 to ascertain the presence of HIC1 (*top panel*: *INPUT*). *D,* HIC1 interacts with the N-terminal moiety of PHF1. A similar co-transfection experiment was performed in HEK293T cells with a similar combination of expression plasmids but using the FLAG-PHF1 encoding amino acids 1–240 corresponding to the conserved functional domains.

detected with HA and MYC antibodies. Our results demonstrate that hPCL3L, but not the hPCL3S isoform lacking the PHD2 domain, promotes interactions between HIC1 and two PRC2 components, EZH2 and SUZ12 (Fig. 5, compare *lanes 6–8*). The strong and constant interaction observed with EED (*lanes 6–8*) could be explained by the interaction between EED and the C-terminal moiety of HIC1 containing the 5 zinc finger motifs (supplemental Fig. S1).

To unambiguously demonstrate that hPCL3L, HIC1, and the PRC2 complex are engaged into a ternary complex, FLAG-HIC1, HA-hPCL3L, and PRC2 components (MYC-EZH2, HA-SUZ12, and HA-EED) were cotransfected in HEK293T cells and we performed two rounds of sequential immunoprecipitation (44). The cell lysates were first immunoprecipitated with FLAG antibodies coupled to agarose beads and the immunoprecipitated proteins were eluted with an excess of FLAG peptide. Then, this eluate was subjected to a second immunoprecipitation step using the polyclonal antibodies directed against hPCL3L (10). Finally, the proteins immunoprecipitated in this second round were analyzed by Western blot with the HA (for SUZ12, hPCL3, and EED), MYC (for EZH2), and HIC1 antibodies. As shown in Fig. 6*A*, we detected a specific ternary complex containing all these proteins (*lane 8*).

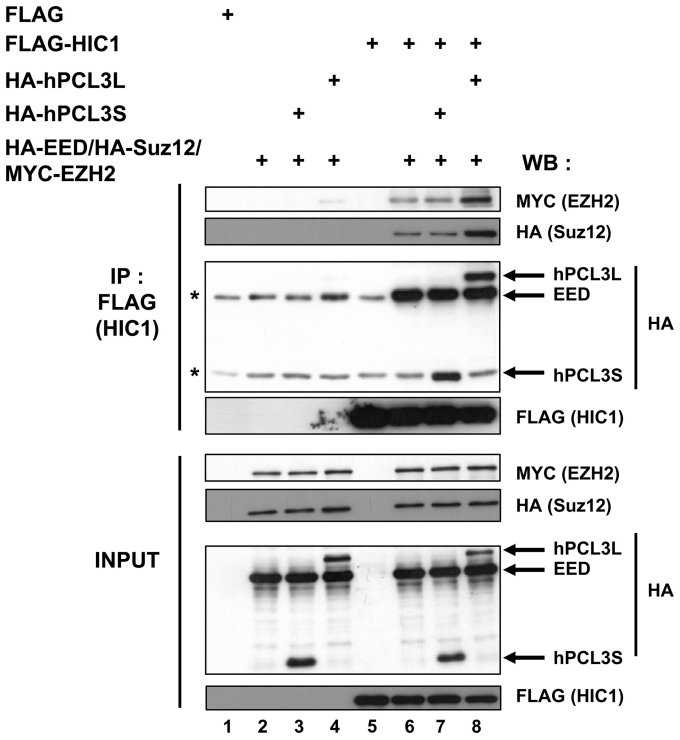

FIGURE 5. **hPCL3L but not hPCL3S promotes the interaction between HIC1 and members of the PRC2 complex.** HEK293T cells were transiently transfected with the indicated expression plasmids as well as with the empty pcDNA3-FLAG vector as a control for 48 h. Whole cells extracts were prepared in IPH buffer and incubated with anti-FLAG antibodies (*top four panels*, *IP*: *FLAG* (*HIC1*), *lanes 1–8*) and immunoblotted (*WB*) with anti-FLAG monoclonal antibodies to verify the presence of HIC1 in the immunoprecipitates (*IP*) and with antibodies against the MYC and HA epitope to detect co-immunoprecipitation, respectively, of EZH2 and Suz12, EED, hPCL3L, and hPCL3S. 2% of each lysate was directly resolved by SDS-PAGE and immunoblotted with the same antibodies to ascertain the presence of the relevant expression vectors in each transfection condition (*bottom four panels*: *INPUT*, *lanes 1–8*).

In accordance with these results, upon ectopic expression in HEK293T, FLAG-HIC1 proteins could efficiently co-immunoprecipitate hPCL3L as well as several endogenous PRC2 components including Suz12, Eed, and EZH2, the catalytic subunit of PRC2 complexes, but not the PRC1 component Bmi1 (Fig. 6*B*). In addition, we were able to detect an interaction between the endogenous HIC1 and Suz12 proteins in WI-38 fibroblasts (Fig. 6*C*). In conclusion, our results suggest that Polycomb-like proteins, and especially hPCL3L, can stabilize interactions between HIC1 and PRC2 components through the formation of a ternary complex.

EZH2 and H3K27 Trimethylation Are Associated with a Subset of HIC1 Target Genes—We then examined if these interactions could result in a functional activity of Polycomb complexes on HIC1 target genes. To that end, we assessed by ChIP-qPCR analyses the levels of two epigenetic marks and the histone methyltransferase EZH2 on various HIC1 target genes in WI-38 cells. The histone modification H3K27me3, specifically catalyzed by PRC2, was detected on canonical PRC2 target genes such as *MYT1*, *CCND2*, and the *ATOH1* enhancer as expected (45), but also on *CXCR7* (37) and *EFNA1* (46), two HIC1 target genes that had not been previously recognized as PCR2 targets (Fig. 7*A*). The *ATOH1* enhancer is a direct target gene of HIC1 in mouse embryonic cerebellum and in human medulloblastoma cell lines (47) as well as in normal WI-38 fibroblasts (27). Interestingly, *ATOH1* is also found in a list of genes repressed by PRC2 components in TIG3 human embryonic fibroblasts (45). By contrast, no consistent level of H3K27me3 modification was detected on other HIC1 target genes such as *CCND1*, the distal sites in the *SIRT1* promoter and *E2F1*, or on the *GAPDH* promoter used as negative control. Previously, we detected through ChIP analyses followed by PCR amplification the presence of H3K27me3 on the proximal HIC1 binding sites in the *SIRT1* promoter (27). However, due to the extremely high GC content of this region, we failed to amplify it in our quantitative ChIP-qPCR assays (data not shown).

In accordance with H3K27me3 detection, EZH2 was highly detected on *MYT1*, *ATOH1*, and *EFNA1* but at lower levels on *CCND2* and *CXCR7* (Fig. 7*B*). Surprisingly, despite the absence of H3K27me3, significant levels of EZH2 were also detected on the distal *SIRT1* promoter (Fig. 7*B*).

We next assessed by ChIP the levels of an activating epigenetic mark on the same subset of genes. As shown in Fig. 7*C*, the levels of H3K27me3 are globally inversely mirrored on each gene by the levels of total acetylated histone H3. In conclusion, several HIC1 target genes are enriched in H3K27me3 histone modification and the PRC2-methyltransferase EZH2 in close agreement with the interaction between HIC1, Polycomb-like proteins, and PRC2.

HIC1 Recruits PHF1 and PRC2 Complex to ATOH1 Enhancer in WI-38 Cells—We next wanted to investigate the relationship between HIC1, human Polycomb-like proteins, and PRC2 complex at an endogenous target locus. To demonstrate that *ATOH1* is indeed a target gene common to the HIC1 and PRC2 complexes, we carried out single ChIP experiments in growing WI-38 cells. As shown in Fig. 8*A*, HIC1 is found at the *ATOH1* enhancer together with the H3K27me3 epigenetic mark specifically deposited by the PRC2 complex. However, we failed to detect any enrichment for hPCL3L. This result suggests that our hPCL3L antibodies, although suitable for ChIP after transient transfection of hPCL3L (data not shown) might not be suitable for ChIP analyses of endogenous proteins. Another explanation could be the relatively low level of *hPCL3*L mRNAs previously detected by qRT-PCR analyses of WI-38 cells (10). Indeed, hPCL3 seems preferentially overexpressed in many cancers (9). Therefore, we investigated the binding of PHF1, which interacts with HIC1 (Fig. 1*D*) and which, by contrast with hPCL3, is strongly expressed in WI-38 cells (10). As expected from all our results, we detected PHF1 bound to the *ATOH1* enhancer together with HIC1 and H3K27me3 (Fig. 8*B*). In addition, these ChIP analyses also demonstrated the binding of EZH2, the catalytic component of PRC2, as well as of Bmi1, a core component of PRC1 to the *ATOH1* enhancer. As control, neither H3K27me3 nor any of these proteins were detected on the *GAPDH* promoter (Fig. 8*B*).

To further confirm that HIC1 recruits PHF1 to the *ATOH1* enhancer, we performed sequential ChIP experiments as previously described (27). Chromatins prepared from WI-38 cells were immunoprecipitated with HIC1 antibodies followed by PHF1 antibodies or rabbit IgG as negative control. As shown in Fig. 8*C* (*left panel*), a PCR-amplified band was obtained only for

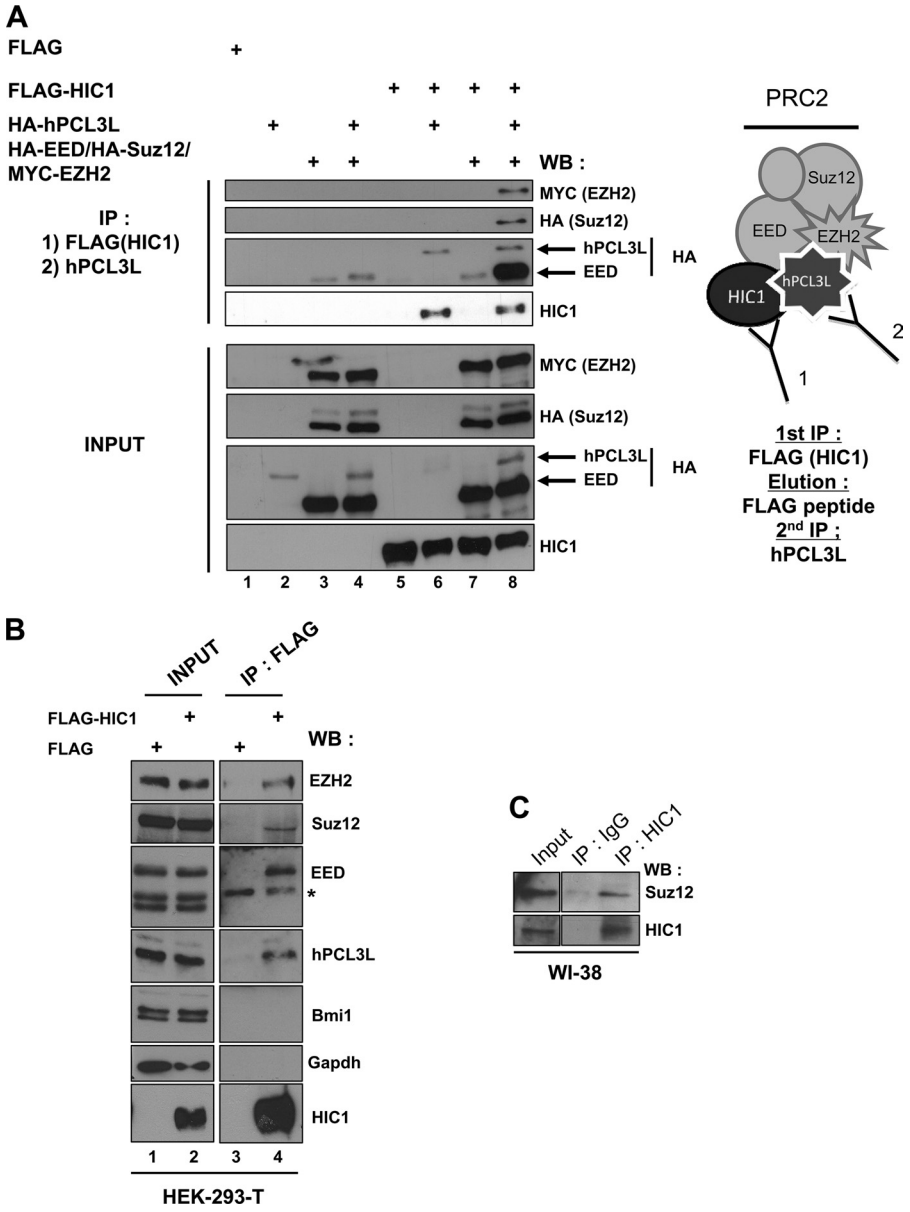

FIGURE 6. **HIC1 forms a ternary complex with hPCL3L and PRC2.** The sequential immunoprecipitation (*IP*) protocol is schematically drawn. HEK293T cells were transiently transfected with the indicated combination of FLAG-HIC1, MYC-EZH2, and HA-tagged versions of hPCL3L, Suz12, or EED as well as with the empty pcDNA3-FLAG vector as a control. Whole cells extracts were prepared in IPH buffer and incubated with anti-FLAG antibodies coupled to agarose beads (*IP*: *FLAG*, *lanes 1–8*). After washings, the beads were incubated with excess FLAG peptide to elute the immunoprecipitated materials, which were then subjected to a second round of immunoprecipitation with anti-hPCL3L antibodies recognizing the transitory expressed but not the endogenous proteins. These immunoprecipitates were immunoblotted (*WB*) with anti-MYC, anti-HA, and anti-HIC1 antibodies to detect the formation of the ternary complex in the relevant immunoprecipitates (*top four panels*, *lanes 1–8*). 2% of each lysate was directly resolved by SDS-PAGE and successively immunoblotted with anti-MYC, anti-HA, and anti-HIC1 antibodies (*INPUT*, *bottom four panels*, *lanes 1–8*). *B*, co-immunoprecipitation analyses of chromatin-associated proteins. HEK293T cells were transfected transiently with the expression vector for FLAG-tagged HIC1 or the empty pcDNA3-FLAG vector as a control. The chromatin-associated fractions were prepared as previously described (10) and incubated with anti-FLAG antibodies. 2% of each nuclear fraction (*INPUT*, *lanes 1* and *2*) and the immunoprecipitates (*IP*: *FLAG*, *lanes 3* and *4*) were directly resolved by SDS-PAGE and transferred to nitrocellulose membranes. Relevant pieces were immunoblotted (*WB*) with monoclonal anti-EZH2, EED, Bmi1, and GAPDH or polyclonal anti-hPCL3L (10) and Suz12 antibodies to detect co-immunoprecipitation of these endogenous proteins with exogenous FLAG-HIC1 (*top two panels* (*IP*: *FLAG*), *lanes 3* and *4*). As control the blot was also probed with anti-FLAG to verify the presence of HIC1 in the INPUT and in the relevant immunoprecipitate (*bottom panels*, *lanes 2* and *4*). *C,* co-immunoprecipitation of endogenous Suz12 proteins by HIC1 in normal WI-38 fibroblasts.

HIC1/PHF1 on the *ATOH1* enhancer. As control, similar results were obtained when we carried out the sequential ChIP with the PHF1 antibodies first (Fig. 8*C*, *right panel*) and no signal was obtained for the *GAPDH* promoter. In conclusion, these results demonstrate that HIC1 might form a stable complex with PHF1 on the *ATOH1* enhancer, which is also co-occupied by PRC2 and PRC1 components.

To directly link the interaction between HIC1 and PHF1 to recruitment of the PRC2 complex, we assessed the levels of EZH2, H3K27me3, and of total acetylated H3 on a subset of target genes in WI-38 cells transfected with siRNA targeting HIC1 or control siRNA. In these cells, protein levels of HIC1 were almost completely extinguished, whereas the total levels of EZH2, H3K27me3, and histone H3 appeared globally unaf-

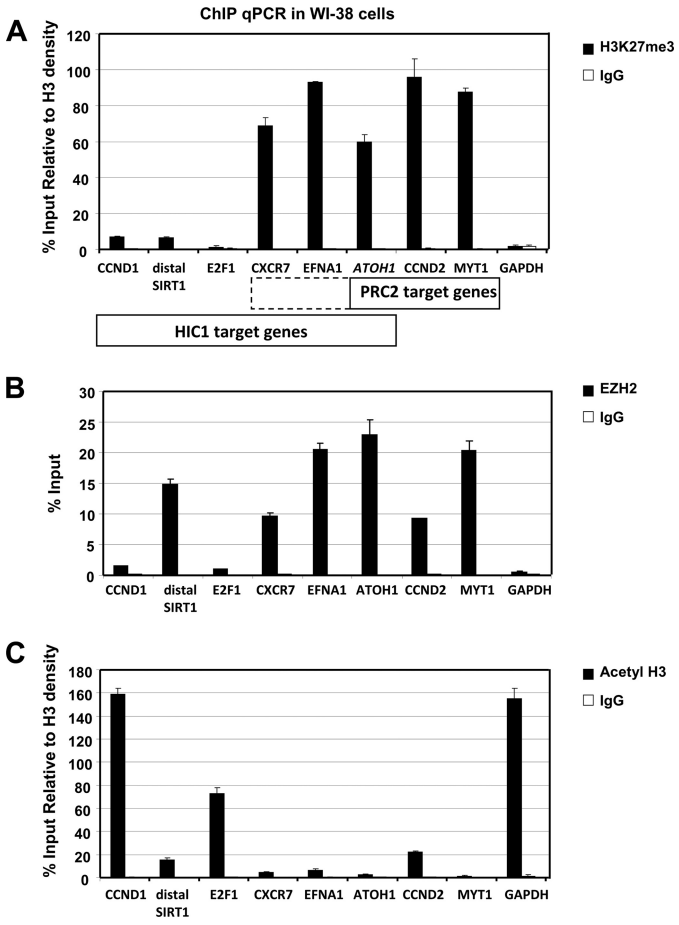

FIGURE 7. **A subset of HIC1 target genes is associated with H3K27 trimethylation and EZH2.** Levels of H3K27 trimethylation (*A*), EZH2 (*B*), and total acetylated H3 (*C*) of various genes were analyzed by ChIP-qPCR in WI-38 fibroblasts. The genes analyzed are arranged in three groups: HIC1 target genes (*CCND1, SIRT1*-distal HiRE sites-, *E2F1*, *CXCR7*, *EFNA1,* and *ATOH1*), *Polycomb* target genes (*ATOH1*, *CCND2,* and *MYT1*), and a housekeeping gene as control (*GAPDH*). The *dotted box* highlights *CXCR7* and *EFNA1*, which have been identified as potential PRC2 target genes in this study due to the presence of H3K27me3 and EZH2. Enrichments for each modification were assessed by quantitative real-time PCR in triplicate. A representative experiment is shown.

fected (Fig. 8*E*). We carried ChIP analyses on *MYT1* as a canonical PCR2 target and on two HIC1 target genes enriched in H3K27me3 and EZH2, *EFNA1* and *ATOH1*, as well as on *GAPDH* as non-binding control (Fig. 7). For *ATOH1*, besides the enhancer sequence we also included in our assays three regions in its promoter containing consensus HIC1 binding sites (Fig. 8*D*) because a genome-wide analyses of *Polycomb* targets indicated that in most cases they were detected within 1 kbp of the transcription start site (48). In these HIC1 knocked-down cells, we observed a significantly reduced occupancy of EZH2 all along the *ATOH1* promoter and on *EFNA1*, whereas the occupancy of *MYT1* remained constant (Fig. 8*F*). Strikingly, despite the reduced binding of the H3K27-specific histone methyltransferase EZH2 on *ATOH1* and *EFNA1*, the levels of H3K27me3 modifications were unaffected (Fig. 8*F*). Furthermore, these genes were not derepressed in HIC1 knock-out cells as measured by qRT-PCR analyses (data not shown). Such a situation is not unprecedented and has been already observed, for example, in embryonic stem cells knocked-down for Pcl2 (15). Nevertheless, total acetyl-H3 levels were significantly increased on the proximal sites of the *ATOH1* promoter (Fig. 8*G*). This could reflect a partial and incomplete activation of these HIC1 and PRC2 target genes, corresponding to the recently characterized antagonistic switch between H3 lysine 27 methylation and acetylation in the transcriptional regulation of *Polycomb* target genes (49).

To consolidate these results, we switched to another cell type expressing high levels of endogenous HIC1, the immortalized foreskin fibroblasts BJ-tert. In these cells, a stable *HIC1* downregulation was obtained by retroviral-induced expression of a specific shRNA (Fig. 9*A*). As expected from our previous results, in the absence of HIC1, we equally observed a significant decrease of EZH2 occupancy all along the *ATOH1* locus (Fig. 9*C*), confirming the implication of HIC1 in PRC2 recruitment. As previously described (12), EZH2 recruitment was not affected in the absence of PHF1 (Fig. 9, *B* and *C*, *sh PHF1*). This could be explained by the constant interaction observed between HIC1 and another PRC2 component EED, independently of PCL proteins (Fig. 5). However, in BJ-tert cells treated with siRNA for a longer period (6 days), H3K27me3 levels on *ATOH1* were slightly diminished in the absence of HIC1, although less efficiently than following EZH2 depletion (Fig. 10).

In conclusion, even though H3K27me3 levels remained only slightly affected, HIC1 depletion strongly reduced PRC2 occupancy on *ATOH1* in two different cell types and by two independent methods of HIC1 knockdown, namely inactivation by siRNAs or shRNAs. These results thus strongly support a functional interaction between the transcriptional repressor HIC1 and *Polycomb-like* proteins in WI-38 and BJ-tert fibroblasts and most likely during embryonic development on a subset of HIC1 target genes.

HIC1 and Polycomb Complexes Are Functionally Linked on ATOH1 during Cerebellum Development in Vivo—We finally decided to validate *in vivo* the new relationship established between HIC1 and Polycomb complexes. For this purpose, we focused on mouse cerebellar development as a dynamic functional model of HIC1-induced repression of *ATOH1*, which is found deregulated in medulloblastomas (47, 50, 51). Briefly, cerebellum is composed of two main cell layers. Postnatal expansion driven by Sonic hedgehog (Shh) of granule cell precursors forms the external granule cell layer composed of proliferative $Brdu^{+}/ATOH1^{+}/HIC1^{--}$ cells (47, 50, 52). After 7 days of cerebellar development, those cells start to differentiate and migrate through the Purkinje cells and the molecular cell layers to form the mature granule cells, which are $BrdU^{-}/ATOH1^{-}/HIC1^{+}$ in the internal granule cell layer (47, 50, 52). P5 and P21 mice cerebellum are, respectively, composed in the majority of proliferating granule cell precursor cells and of differentiated mature granule cell cells. Postnatal cerebella were dissected from P5 and P21 mice and *ATOH1* repression during development was confirmed by qRT-PCR in P21 cerebellum (Fig. 11*A*, *top panel*) in accordance with HIC1 binding on its enhancer as previously described (47) and hereby demonstrated by ChIP (Fig. 11*A*, *bottom panel*). Finally, to extend these results in line with our model, epigenetic mark

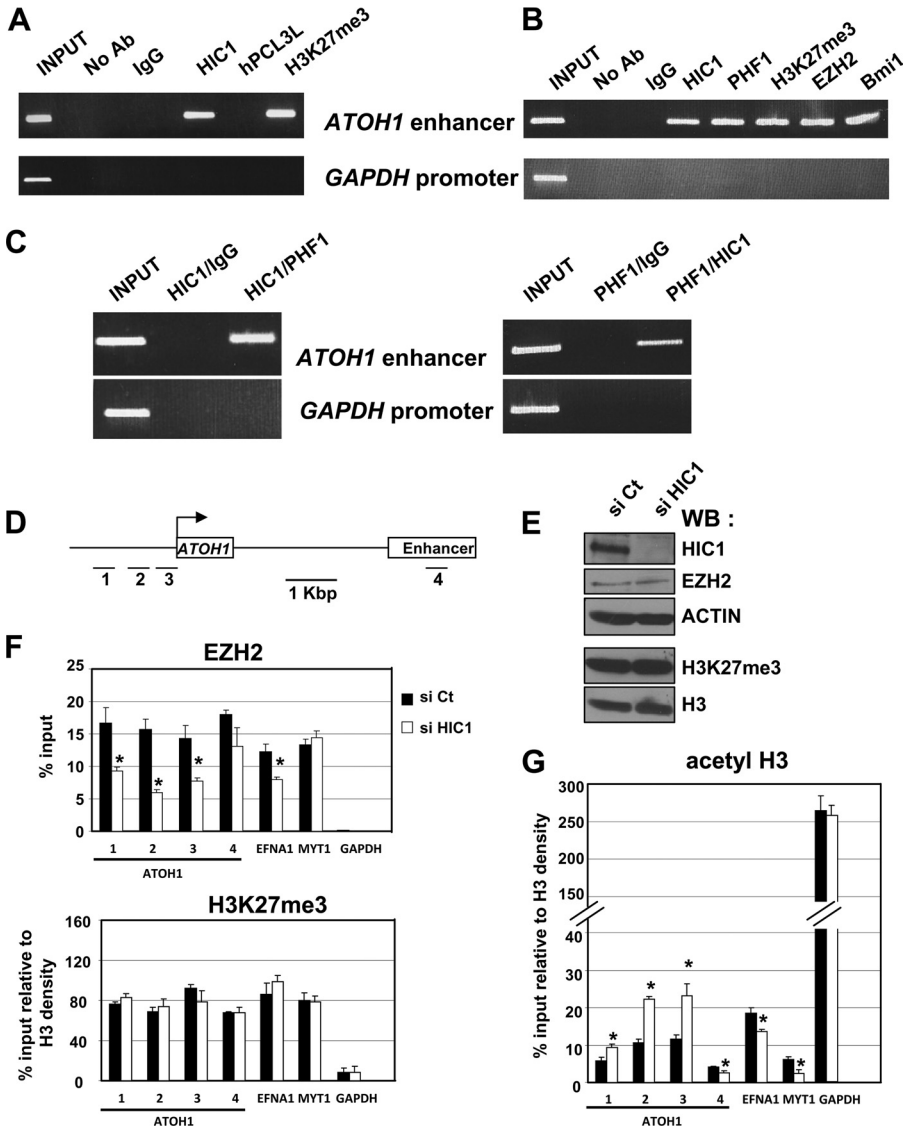

FIGURE 8. **EZH2 recruitment on *ATOH1* and *EFNA1* is HIC1-dependent in WI-38 fibroblasts.** *A*, *ATOH1* is a target gene common to HIC1 and PRC2 but not to hPCL3. Human WI-38 fibroblasts were analyzed by single ChIP with the indicated antibodies. PCR amplifications were performed with primers flanking the functional HiREs identified in the *ATOH1* enhancer. PCR with the 5′ promoter of *GAPDH* was used as an internal nonbinding control. *B*, HIC1 co-localizes with PHF1 and *Polycomb* complexes at the *ATOH1* enhancer in WI-38 fibroblasts. Human WI-38 fibroblasts were analyzed by single ChIP with the indicated antibodies as described above. *C*, ChIP upon ChIP assays demonstrate that HIC1 and PHF1 might form a stable complex on the *ATOH1* enhancer. Sequential ChIP analyses were performed on WI-38 cells using either anti-HIC1 (*left panel*) or anti-PHF1 (*right panel*) antibodies for the first IP. After this first IP, the bound material was eluted, divided in two, and subjected to a second round of immunoprecipitation, respectively, with anti-PHF1 and anti-HIC1 antibodies or non-immune rabbit IgG as control. PCR amplifications were performed as described above. *D*, schematic drawing of the *ATOH1* locus. The unique exon and the enhancer, as described under accession number NM_005712 (gi4885074), are drawn to scale. The positions of the primers used to amplify PCR regions containing potential HIC1 consensus binding sites in the promoter (*1* to *3*) and in the enhancer (*4*) are indicated *below*. *E*, inactivation of endogenous *HIC1* in WI-38 fibroblasts. WI-38 cells were transfected with non-target siRNA control or with *HIC1* siRNA and whole cell extracts were analyzed by Western blotting for the expression levels of HIC1, EZH2, H3K27me3, and total H3. Actin was used as a loading control. *F*, recruitment of EZH2 and levels of H3K27me3 modifications on two HIC1 target genes, *ATOH1* and *EFNA1*, were analyzed by ChIP in WI-38 cells transfected with non-target siRNA control or with *HIC1* siRNA. *MYT1* and *GAPDH* were analyzed similarly, respectively, as a *Polycomb* target gene and as a control housekeeping gene. Enrichments for EZH2 and H3K27me3 modification were assessed by quantitative real-time PCR in triplicate. *G*, levels of acetyl-H3 were analyzed as described above. *Asterisk* (*) indicates $p < 0.05$.

occupancy on *ATOH1* were addressed by ChIP-qPCR. As expected from all of our results, in P21 mouse cerebellum, we observed a significant increase of H3K27me3 levels and a concomitant diminution of acetyl-H3 and H3K27me2 levels (Fig. 11, *B* and *C*).

These results confirmed *in vivo* the functional interaction between HIC1 and Polycomb complexes first described *in vitro* through an original mechanism involving Polycomb-like proteins and second, *ex vivo* in WI-38 and BJ-tert cells where HIC1 is necessary for the stable recruitment of the PRC2 complex on a subset of its target genes.

DISCUSSION

In this report, we identified human Polycomb-like proteins, hPCL3 and PHF1, as new HIC1 corepressors. These findings decipher another transcriptional repression mechanism selectively brought about by HIC1 on a subset of its target genes. More generally, we demonstrate for the first time that a

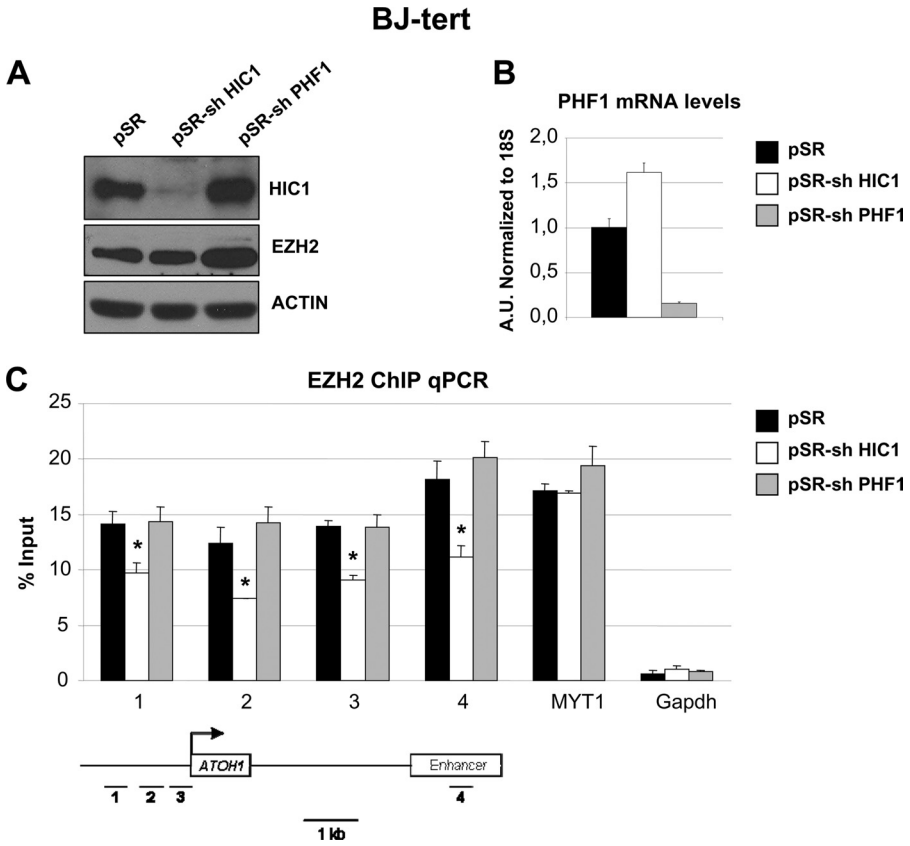

FIGURE 9. **EZH2 recruitment on *ATOH1* is also HIC1-dependent in BJ-tert fibroblasts.** Inactivation of endogenous *HIC1* or *PHF1* in BJ-tert fibroblasts. BJ-tert cells were infected with the control pSR vector or with pSR-*HIC1* shRNA or pSR-*PHF1* shRNA. In *A*, whole cell extracts were analyzed by Western blotting for the expression levels of HIC1 and EZH2. Actin was used as a loading control. In *B, PHF1* mRNA levels were assessed by quantitative RT-PCR. In *C*, EZH2 enrichment was evaluated by ChIP qPCR on *ATOH1*, *MYT1*, and *GAPDH* as described above. The *asterisk* (*) indicates $p < 0.05$.

sequence-specific transcription factor interact with Polycomb-like proteins in mammals to favor the recruitment of PCR2 to some of its target genes.

Through yeast two-hybrid screening of a human mammary gland library with the two HIC1 repression domains, BTB-RC, as a bait, we have previously identified the SWI/SNF, CtBP, and NuRD complexes as HIC1 corepressors (27, 32). For these latter two, we have identified two small conserved peptide motifs located in the central region as being involved in the interaction (27, 31, 42). Here, we have validated through various biochemical assays another candidate isolated in the same screen, hPCL3. Interestingly, the interaction between HIC1 and hPCL3 relies mainly on the HIC1 BTB/POZ domain. The BTB/POZ domain is a conserved dimerization and protein/protein interaction domain found in multiple proteins throughout eukaryotic genomes (53, 54). In human, more than 50 proteins contain an N-terminal BTB/POZ domain associated with Krüppel zinc fingers. Most of them are transcriptional repressors that recruit HDAC containing complexes mainly through their BTB/POZ domain, such as for example, BCL6 and PLZF, respectively, implicated in diffuse large B-cell lymphomas and in acute promyelocytic leukemias. By contrast, HIC1 BTB/POZ is a repression domain independent of Class I and Class II HDAC whose repression mechanisms are still elusive (43). Although HIC1 interacts, at least partly through its BTB/POZ domain, with Class III HDAC SIRT1 (20), this interaction could be rather involved in the regulation of HIC1 transcriptional activity through the acetylation/SUMOylation switch on lysine 314 favoring NuRD recruitment (27, 33). Therefore, our results provide the first mechanistic clue for the repression function of the HIC1 BTB/POZ domain. Notably, the PLZF BTB/POZ domain also interacts with the Polycomb group protein Bmi1, a component of the PRC1 complex (55). Although we cannot totally exclude the participation of the central region, our results demonstrate that the interaction between HIC1 and hPCL3 occurred independently of the CtBP and NuRD complexes. These findings fit perfectly with the model of the hierarchical recruitment of repressing complexes, with HDACs containing complexes first, followed by Polycomb complexes to establish a robust epigenetic silencing of some target genes (55).

Reciprocally, we demonstrate that HIC1 interacts with two domains found in the N-terminal functional module conserved between hPCL3L and PHF1, the TUDOR and PHD2 domains. The TUDOR domain initially characterized in RNA-binding protein is now widely recognized as a domain essential for transcriptional regulation through its binding implicating a cage of 2 to 4 aromatic residues to methylated lysine or arginine in various proteins, including histone tails (56–58). However, a recent NMR study of the *Drosophila* Polycomb-like TUDOR domain revealed that it contained an atypical incomplete "aromatic cage" unlikely to bind methylated lysine or arginine. By contrast, the human PCL orthologs exhibit a complete aromatic cage and might thus bind methylated residues (59). In addition, *Drosophila* and human PCL proteins share a distinct

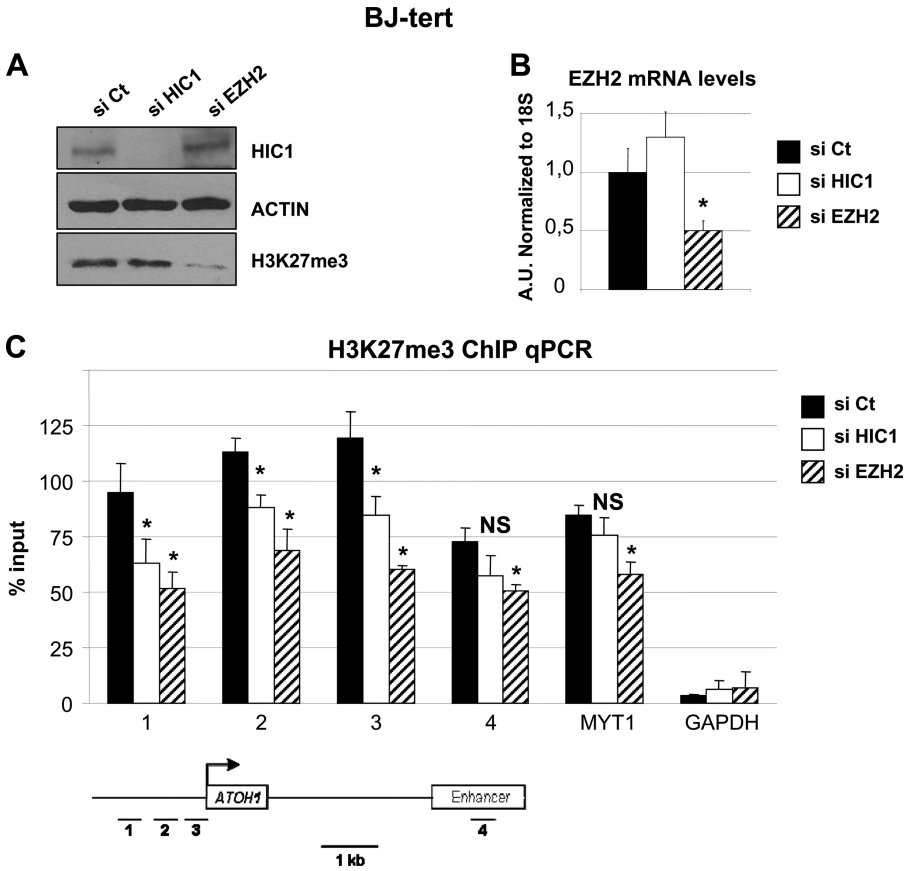

FIGURE 10. **Extended loss of *HIC1* affects H3K27me3 levels on ATOH1 in BJ-tert fibroblasts.** Inactivation of endogenous *HIC1* or *EZH2* in BJ-tert fibroblasts with siRNA treatment for 6 days. In *A*, whole cell extracts were analyzed by Western blotting for the expression levels of HIC1 and H3K27me3. Actin was used as a loading control. In *B*, EZH2 mRNA levels were assessed by qRT-PCR. In *C*, enrichments for H3K27me3 modification were assessed by ChIP qPCR on *ATOH1*, *MYT1*, and *GAPDH* as described above. The *asterisk* (*) indicates $p < 0.05$.

hydrophobic patch at the surface of their TUDOR domains that could be engaged in protein-protein interactions (59), as shown here for HIC1 and previously for EZH2 (10). Finally, the TUDOR domain is also common to the two hPCL3 isoforms, which exhibit different subcellular localization and belong to different high-molecular weight complexes containing at least EZH2 (10). Therefore, regardless of the final composition and physiological function of these two isoform-specific hPCL3 containing complexes, HIC1 can interact with both of them but the physiological relevance of the interaction between HIC1 and the short isoform of hPCL3 still remains elusive.

Another domain implicated in the interaction with HIC1 is the PHD2 domain. The PHD finger originally characterized as a protein-protein interaction domain is involved in many biochemical functions, notably methyl-lysine binding (60, 61). Its PHD2 domain appears essential for the function of hPCL3 proteins because it is also implicated in the interaction with EZH2 as well as in the self-association of hPCL3L (10). Furthermore, the PHD2 domain of Pcl2 is required for PRC2 targeting in embryonic stem cells (15). Given the high sequence homology in their PHD2 domains, these functional properties might be shared by all human Polycomb-like paralogs. According to the cross-brace model predicted from several structural analyses of PHD fingers (60), this PHD2 domain could be engaged simultaneously in interactions with several partners. It is tempting to speculate that transcription factors could participate in and/or even stabilize this interaction through concomitant interaction with the PHD2 domains of hPCL proteins.

The mechanisms involved in the targeting of the Polycomb complexes to their target loci display salient differences between *Drosophila* and mammals (62, 63). PcG proteins do not have the ability to bind to DNA except for the recently characterized JARID2 co-factor in embryonic stem cells (4, 5). In *Drosophila*, several transcription factors such as YY1, GAGA factor, or Zeste are required to recruit PcG proteins to *cis*-acting regions called Polycomb repressive elements. Whereas several genomewide mapping studies of PcG binding sites in mammals have been performed (45, 48), no Polycomb repressive elements have been identified in mammals, except in two studies (64, 65). Therefore, several mammalian transcription factors are supposed to recruit PcG proteins to specific loci (1, 62). For example, the PML-RARα and PLZF-RARα chimeric fusion proteins implicated in acute promyelocytic leukemia interact, respectively, with PRC2 components EZH2 and SUZ12 (66) and with the PRC1 component Bmi1 (55). Similarly, the Snail1 transcription factor represses *E-cadherin* expression through interaction via SUZ12 and EZH2 (67). Despite these numerous examples, HIC1 is, to the best of our knowledge, the first transcription factor shown to interact with human Polycomb-like proteins.

However, their exact functions still remain elusive. According to studies in *Drosophila* and mammals, they are involved in

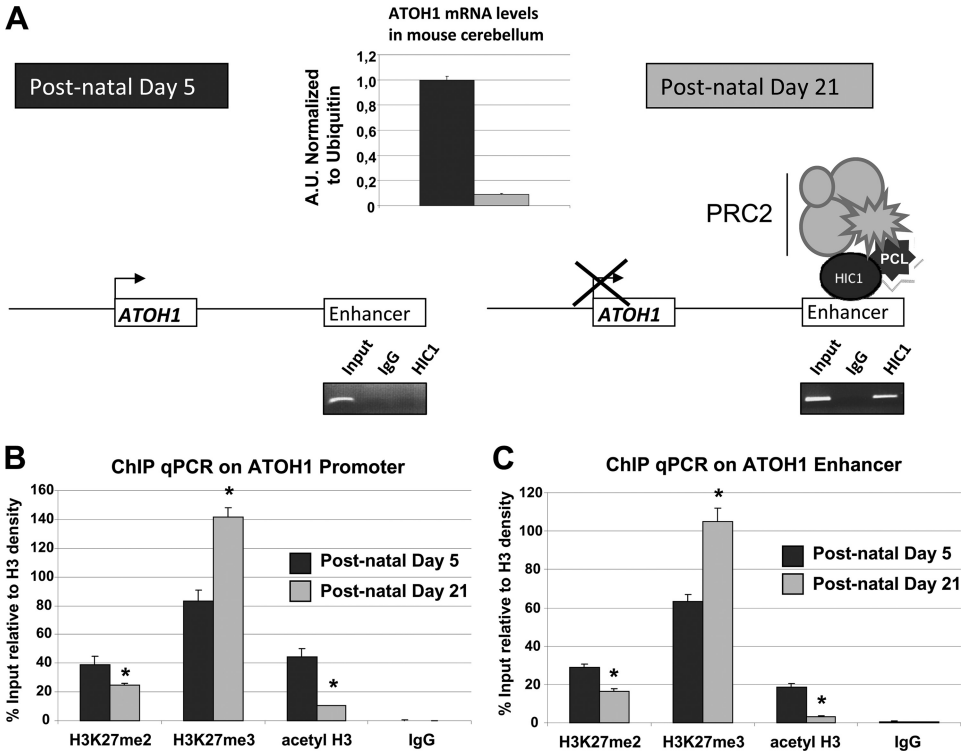

FIGURE 11. **HIC1 and Polycomb complexes are functionally linked on *ATOH1* during mouse cerebellum development *in vivo*.** Postnatal cerebella were dissected from P5 and P21 C57BL/6 mice. In *A*, *ATOH1* mRNA levels were analyzed by quantitative RT-PCR (*top panel*) and HIC1 binding on *ATOH1* enhancer was assessed by ChIP (*bottom panel*). The *middle panel* schematically describes the model of Polycomb recruitment by HIC1 on *ATOH1* during cerebellar development. In *B* and *C*, levels of H3K27 di- and trimethylation and total acetylated H3 were analyzed by ChIP-qPCR on *ATOH1* promoter (*B*) and enhancer (*C*). The *asterisk* (*) indicates $p < 0.05$.

recruitment and/or activation of PRC2 (8, 11–15). Our results suggest their implication in the recruitment or stabilization of PRC2 by the transcription factor HIC1.

In our experimental conditions, PRC2 levels were only partly reduced in the absence of HIC1, suggesting that other factors could be involved in their recruitment in addition to HIC1, the latter allowing its stabilization by recruiting Polycomb-like proteins. Following HIC1 decreases, PRC2 could also be maintained at least for a short time on their common target genes, notably by a direct interaction of the EED protein with H3K27me3 (3, 68). Then H3K27me3 could be maintained and this could explain the absence of derepression of target loci as previously reported following knockdown of PCL2 in embryonic stem cells (15). Polycomb target genes are stably repressed and even after the loss of PRC2 components, their re-expression is not obviously observed (48, 69).

HIC1 is a tumor suppressor gene also implicated in normal development (17, 18, 24). Despite its functional importance, very few HIC1 direct target genes have been identified so far. Among them, we have demonstrated the PRC2 recruitment, as assessed by EZH2 co-occupancy and high levels of H3K27 trimethylation, on *ATOH1*, *EFNA1*, and *CXCR7*. *ATOH1*, a proneuronal transcription factor, essential for migration of granule cell precursors during cerebellum development, has already been identified as a PRC2 target gene in TIG3 human embryonic fibroblasts (45). HIC1 is dynamically regulated through the migration of the granule cell precursors into the internal granule cell layer (47). In addition, loss of HIC1 through hypermethylation of its promoters is often found in medulloblastomas (70). Therefore, the efficient repression of *ATOH1* and possibly other targets by HIC1 through PRC2 is intimately linked to cerebellar differentiation and required to avoid tumorigenesis. *CXCR7*, a scavenger receptor for the chemokine SDF-1 is up-regulated in breast, lung, and prostate tumors, which often display *HIC1* hypermethylation (32). Similarly, *EFNA1*, which encodes a cell surface ligand for Eph tyrosine kinase receptors, is a direct target gene of HIC1 whose deregulation through *HIC1* epigenetic silencing contributes to epithelial malignancy (46). *CXCR7* (71, 72) and *EFNA1* (46, 73) have also been implicated in proper embryonic development.

In conclusion, HIC1 has been implicated in normal development as well as in cellular growth (27, 29, 30, 46) whose deregulation due to HIC1 loss could contribute to tumorigenesis. Thus, the functional interaction of HIC1 with the PRC2 complex in cancer and development remains to be investigated. It will also be essential to decipher the precise mechanisms underlying the differential promoter binding by the various HIC1-corepressors complexes. These studies will help to decipher the roles of *HIC1* in development as well as the mechanisms underlying its tumor suppressor function.

Acknowledgments—We thank Dr. Raphaël Margueron for helpful discussions and Dr. Brian R. Rood for critical reading of the manuscript.

REFERENCES

1. Sauvageau, M., and Sauvageau, G. (2010) Polycomb group proteins. Multifaceted regulators of somatic stem cells and cancer. *Cell Stem Cell* **7**,

299–313
2. Morey, L., and Helin, K. (2010) Polycomb group protein-mediated repression of transcription. *Trends Biochem. Sci.* **35,** 323–332
3. Margueron, R., and Reinberg, D. (2011) The Polycomb complex PRC2 and its mark in life. *Nature* **469,** 343–349
4. Pasini, D., Cloos, P. A., Walfridsson, J., Olsson, L., Bukowski, J. P., Johansen, J. V., Bak, M., Tommerup, N., Rappsilber, J., and Helin, K. (2010) JARID2 regulates binding of the Polycomb repressive complex 2 to target genes in ES cells. *Nature* **464,** 306–310
5. Li, G., Margueron, R., Ku, M., Chambon, P., Bernstein, B. E., and Reinberg, D. (2010) Jarid2 and PRC2, partners in regulating gene expression. *Genes Dev.* **24,** 368–380
6. Tie, F., Prasad-Sinha, J., Birve, A., Rasmuson-Lestander, A., and Harte, P. J. (2003) A 1-megadalton ESC/E(Z) complex from *Drosophila* that contains Polycomb-like and RPD3. *Mol. Cell. Biol.* **23,** 3352–3362
7. Coulson, M., Robert, S., Eyre, H. J., and Saint, R. (1998) The identification and localization of a human gene with sequence similarity to Polycomb-like of *Drosophila melanogaster*. *Genomics* **48,** 381–383
8. Walker, E., Chang, W. Y., Hunkapiller, J., Cagney, G., Garcha, K., Torchia, J., Krogan, N. J., Reiter, J. F., and Stanford, W. L. (2010) Polycomb-like 2 associates with PRC2 and regulates transcriptional networks during mouse embryonic stem cell self-renewal and differentiation. *Cell Stem Cell* **6,** 153–166
9. Wang, S., Robertson, G. P., and Zhu, J. (2004) A novel human homologue of *Drosophila* Polycomb-like gene is up-regulated in multiple cancers. *Gene* **343,** 69–78
10. Boulay, G., Rosnoblet, C., Guérardel, C., Angrand, P. O., and Leprince, D. (2011) Functional characterization of human Polycomb-like 3 isoforms identifies them as components of distinct EZH2 protein complexes. *Biochem. J.* **434,** 333–342
11. Nekrasov, M., Klymenko, T., Fraterman, S., Papp, B., Oktaba, K., Köcher, T., Cohen, A., Stunnenberg, H. G., Wilm, M., and Müller, J. (2007) Pcl-PRC2 is needed to generate high levels of H3K27 trimethylation at Polycomb target genes. *EMBO J.* **26,** 4078–4088
12. Sarma, K., Margueron, R., Ivanov, A., Pirrotta, V., and Reinberg, D. (2008) Ezh2 requires PHF1 to efficiently catalyze H3 lysine 27 trimethylation *in vivo*. *Mol. Cell. Biol.* **28,** 2718–2731
13. Cao, R., Wang, H., He, J., Erdjument-Bromage, H., Tempst, P., and Zhang, Y. (2008) Role of hPHF1 in H3K27 methylation and *Hox* gene silencing. *Mol. Cell. Biol.* **28,** 1862–1872
14. Savla, U., Benes, J., Zhang, J., and Jones, R. S. (2008) Recruitment of *Drosophila* Polycomb group proteins by Polycomb-like, a component of a novel protein complex in larvae. *Development* **135,** 813–817
15. Casanova, M., Preissner, T., Cerase, A., Poot, R., Yamada, D., Li, X., Appanah, R., Bezstarosti, K., Demmers, J., Koseki, H., and Brockdorff, N. (2011) Polycomb-like 2 facilitates the recruitment of PRC2 Polycomb group complexes to the inactive X chromosome and to target loci in embryonic stem cells. *Development* **138,** 1471–1482
16. Wales, M. M., Biel, M. A., el Deiry, W., Nelkin, B. D., Issa, J. P., Cavenee, W. K., Kuerbitz, S. J., and Baylin, S. B. (1995) p53 activates expression of HIC-1, a new candidate tumor suppressor gene on 17p13.3. *Nat. Med.* **1,** 570–577
17. Fleuriel, C., Touka, M., Boulay, G., Guérardel, C., Rood, B. R., and Leprince, D. (2009) HIC1 (hypermethylated in cancer 1) epigenetic silencing in tumors. *Int. J. Biochem. Cell Biol.* **41,** 26–33
18. Chen, W. Y., Zeng, X., Carter, M. G., Morrell, C. N., Chiu Yen, R. W., Esteller, M., Watkins, D. N., Herman, J. G., Mankowski, J. L., and Baylin, S. B. (2003) Heterozygous disruption of Hic1 predisposes mice to a gender-dependent spectrum of malignant tumors. *Nat. Genet.* **33,** 197–202
19. Chen, W., Cooper, T. K., Zahnow, C. A., Overholtzer, M., Zhao, Z., Ladanyi, M., Karp, J. E., Gokgoz, N., Wunder, J. S., Andrulis, I. L., Levine, A. J., Mankowski, J. L., and Baylin, S. B. (2004) Epigenetic and genetic loss of Hic1 function accentuates the role of p53 in tumorigenesis. *Cancer Cell* **6,** 387–398
20. Chen, W. Y., Wang, D. H., Yen, R. C., Luo, J., Gu, W., and Baylin, S. B. (2005) Tumor suppressor HIC1 directly regulates SIRT1 to modulate p53-dependent DNA-damage responses. *Cell* **123,** 437–448
21. Jenal, M., Trinh, E., Britschgi, C., Britschgi, A., Roh, V., Vorburger, S. A., Tobler, A., Leprince, D., Fey, M. F., Helin, K., and Tschan, M. P. (2009) The tumor suppressor gene hypermethylated in cancer 1 is transcriptionally regulated by E2F1. *Mol. Cancer Res.* **7,** 916–922
22. Wang, C., Chen, L., Hou, X., Li, Z., Kabra, N., Ma, Y., Nemoto, S., Finkel, T., Gu, W., Cress, W. D., and Chen, J. (2006) Interactions between E2F1 and SirT1 regulate apoptotic response to DNA damage. *Nat. Cell Biol.* **8,** 1025–1031
23. Dehennaut, V., and Leprince, D. (2009) Implication of HIC1 (hypermethylated in cancer 1) in the DNA damage response. *Bull. Cancer* **96,** E66–72
24. Carter, M. G., Johns, M. A., Zeng, X., Zhou, L., Zink, M. C., Mankowski, J. L., Donovan, D. M., and Baylin, S. B. (2000) Mice deficient in the candidate tumor suppressor gene *Hic1* exhibit developmental defects of structures affected in the Miller-Dieker syndrome. *Hum. Mol. Genet.* **9,** 413–419
25. Pospichalova, V., Tureckova, J., Fafilek, B., Vojtechova, M., Krausova, M., Lukas, J., Sloncova, E., Takacova, S., Divoky, V., Leprince, D., Plachy, J., and Korinek, V. (2011) Generation of two modified mouse alleles of the *Hic1* tumor suppressor gene. *Genesis* **49,** 142–151
26. Pinte, S., Stankovic-Valentin, N., Deltour, S., Rood, B. R., Guérardel, C., and Leprince, D. (2004) The tumor suppressor gene *HIC1* (hypermethylated in cancer 1) is a sequence-specific transcriptional repressor. Definition of its consensus binding sequence and analysis of its DNA binding and repressive properties. *J. Biol. Chem.* **279,** 38313–38324
27. Van Rechem, C., Boulay, G., Pinte, S., Stankovic-Valentin, N., Guérardel, C., and Leprince, D. (2010) Differential regulation of *HIC1* target genes by CtBP and NuRD, via an acetylation/SUMOylation switch, in quiescent versus proliferating cells. *Mol. Cell. Biol.* **30,** 4045–4059
28. Mohammad, H. P., Zhang, W., Prevas, H. S., Leadem, B. R., Zhang, M., Herman, J. G., Hooker, C. M., Watkins, D. N., Karim, B., Huso, D. L., and Baylin, S. B. (2011) Loss of a single Hic1 allele accelerates polyp formation in Apc(Δ716) mice. *Oncogene* **30,** 2659–2669
29. Foveau, B., Boulay, G., Pinte, S., Van Rechem, C., Rood, B. R., and Leprince, D. (2012) The receptor tyrosine kinase *EphA2* is a direct target gene of Hypermethylated in Cancer 1 (HIC1). *J. Biol. Chem.* **287,** 5366–5378
30. Boulay, G., Malaquin, N., Loison, I., Foveau, B., Van Rechem, C., Rood, B. R., Pourtier, A., and Leprince, D. (2012) Loss of Hypermethylated in Cancer 1 (HIC1) in breast cancer cells contributes to stress induced migration and invasion through β-2 adrenergic receptor (ADRB2) misregulation. *J. Biol. Chem.* **287,** 5379–5389
31. Deltour, S., Pinte, S., Guerardel, C., Wasylyk, B., and Leprince, D. (2002) The human candidate tumor suppressor gene *HIC1* recruits CtBP through a degenerate GLDLSKK motif. *Mol. Cell. Biol.* **22,** 4890–4901
32. Van Rechem, C., Boulay, G., and Leprince, D. (2009) HIC1 interacts with a specific subunit of SWI/SNF complexes, ARID1A/BAF250A. *Biochem. Biophys. Res. Commun.* **385,** 586–590
33. Stankovic-Valentin, N., Deltour, S., Seeler, J., Pinte, S., Vergoten, G., Guérardel, C., Dejean, A., and Leprince, D. (2007) An acetylation/deacetylation-SUMOylation switch through a phylogenetically conserved psiKXEP motif in the tumor suppressor HIC1 regulates transcriptional repression activity. *Mol. Cell. Biol.* **27,** 2661–2675
34. Laible, G., Wolf, A., Dorn, R., Reuter, G., Nislow, C., Lebersorger, A., Popkin, D., Pillus, L., and Jenuwein, T. (1997) Mammalian homologues of the Polycomb group gene enhancer of zeste mediate gene silencing in *Drosophila* heterochromatin and at *S. cerevisiae* telomeres. *EMBO J.* **16,** 3219–3232
35. Pasini, D., Bracken, A. P., Jensen, M. R., Lazzerini Denchi, E., and Helin, K. (2004) Suz12 is essential for mouse development and EZH2 histone methyltransferase activity. *EMBO J.* **23,** 4061–4071
36. Bracken, A. P., Pasini, D., Capra, M., Prosperini, E., Colli, E., and Helin, K. (2003) EZH2 is downstream of the pRB-E2F pathway, essential for proliferation and amplified in cancer. *EMBO J.* **22,** 5323–5335
37. Van Rechem, C., Rood, B. R., Touka, M., Pinte, S., Jenal, M., Guérardel, C., Ramsey, K., Monté, D., Bégue, A., Tschan, M. P., Stephan, D. A., and Leprince, D. (2009) Scavenger chemokine (CXC motif) receptor 7 (*CXCR7*) is a direct target gene of HIC1 (hypermethylated in cancer 1). *J. Biol. Chem.* **284,** 20927–20935
38. Dahl, J. A., and Collas, P. (2007) Q2 ChIP, a quick and quantitative chromatin immunoprecipitation assay, unravels epigenetic dynamics of devel-

opmentally regulated genes in human carcinoma cells. *Stem Cells* **25,** 1037–1046
39. Srinivasan, L., and Atchison, M. L. (2004) YY1 DNA binding and PcG recruitment requires CtBP. *Genes Dev.* **18,** 2596–2601
40. Morey, L., Brenner, C., Fazi, F., Villa, R., Gutierrez, A., Buschbeck, M., Nervi, C., Minucci, S., Fuks, F., and Di Croce, L. (2008) MBD3, a component of the NuRD complex, facilitates chromatin alteration and deposition of epigenetic marks. *Mol. Cell. Biol.* **28,** 5912–5923
41. Reynolds, N., Salmon-Divon, M., Dvinge, H., Hynes-Allen, A., Balasooriya, G., Leaford, D., Behrens, A., Bertone, P., and Hendrich, B. (2011) NuRD-mediated deacetylation of H3K27 facilitates recruitment of Polycomb repressive complex 2 to direct gene repression. *EMBO J.* **31,** 593–605
42. Stankovic-Valentin, N., Verger, A., Deltour-Balerdi, S., Quinlan, K. G., Crossley, M., and Leprince, D. (2006) A L225A substitution in the human tumor suppressor HIC1 abolishes its interaction with the corepressor CtBP. *FEBS J.* **273,** 2879–2890
43. Deltour, S., Guerardel, C., and Leprince, D. (1999) Recruitment of SMRT/N-CoR-mSin3A-HDAC-repressing complexes is not a general mechanism for BTB/POZ transcriptional repressors, The case of HIC-1 and γFBP-B. *Proc. Natl. Acad. Sci. U.S.A.* **96,** 14831–14836
44. Long, J., Wang, G., Matsuura, I., He, D., and Liu, F. (2004) Activation of Smad transcriptional activity by protein inhibitor of activated STAT3 (PIAS3). *Proc. Natl. Acad. Sci. U.S.A.* **101,** 99–104
45. Bracken, A. P., Dietrich, N., Pasini, D., Hansen, K. H., and Helin, K. (2006) Genome-wide mapping of Polycomb target genes unravels their roles in cell fate transitions. *Genes Dev.* **20,** 1123–1136
46. Zhang, W., Zeng, X., Briggs, K. J., Beaty, R., Simons, B., Chiu Yen, R. W., Tyler, M. A., Tsai, H. C., Ye, Y., Gesell, G. S., Herman, J. G., Baylin, S. B., and Watkins, D. N. (2010) A potential tumor suppressor role for Hic1 in breast cancer through transcriptional repression of ephrin-A1. *Oncogene* **29,** 2467–2476
47. Briggs, K. J., Corcoran-Schwartz, I. M., Zhang, W., Harcke, T., Devereux, W. L., Baylin, S. B., Eberhart, C. G., and Watkins, D. N. (2008) Cooperation between the Hic1 and Ptch1 tumor suppressors in medulloblastoma. *Genes Dev.* **22,** 770–785
48. Boyer, L. A., Plath, K., Zeitlinger, J., Brambrink, T., Medeiros, L. A., Lee, T. I., Levine, S. S., Wernig, M., Tajonar, A., Ray, M. K., Bell, G. W., Otte, A. P., Vidal, M., Gifford, D. K., Young, R. A., and Jaenisch, R. (2006) Polycomb complexes repress developmental regulators in murine embryonic stem cells. *Nature* **441,** 349–353
49. Pasini, D., Malatesta, M., Jung, H. R., Walfridsson, J., Willer, A., Olsson, L., Skotte, J., Wutz, A., Porse, B., Jensen, O. N., and Helin, K. (2010) Characterization of an antagonistic switch between histone H3 lysine 27 methylation and acetylation in the transcriptional regulation of Polycomb group target genes. *Nucleic Acids Res.* **38,** 4958–4969
50. Briggs, K. J., Eberhart, C. G., and Watkins, D. N. (2008) Just say no to ATOH. How HIC1 methylation might predispose medulloblastoma to lineage addiction. *Cancer Res.* **68,** 8654–8656
51. Ayrault, O., Zhao, H., Zindy, F., Qu, C., Sherr, C. J., and Roussel, M. F. (2010) Atoh1 inhibits neuronal differentiation and collaborates with Gli1 to generate medulloblastoma-initiating cells. *Cancer Res.* **70,** 5618–5627
52. Grimmer, M. R., and Weiss, W. A. (2008) BMPs oppose Math1 in cerebellar development and in medulloblastoma. *Genes Dev.* **22,** 693–699
53. Albagli, O., Dhordain, P., Deweindt, C., Lecocq, G., and Leprince, D. (1995) The BTB/POZ domain. A new protein-protein interaction motif common to DNA- and actin-binding proteins. *Cell Growth Differ.* **6,** 1193–1198
54. Stogios, P. J., Downs, G. S., Jauhal, J. J., Nandra, S. K., and Privé, G. G. (2005) Sequence and structural analysis of BTB domain proteins. *Genome Biol.* **6,** R82
55. Boukarabila, H., Saurin, A. J., Batsché, E., Mossadegh, N., van Lohuizen, M., Otte, A. P., Pradel, J., Muchardt, C., Sieweke, M., and Duprez, E. (2009) The PRC1 Polycomb group complex interacts with PLZF/RARA to mediate leukemic transformation. *Genes Dev.* **23,** 1195–1206
56. Adams-Cioaba, M. A., and Min, J. (2009) Structure and function of histone methylation binding proteins. *Biochem. Cell Biol.* **87,** 93–105
57. Huang, Y., Fang, J., Bedford, M. T., Zhang, Y., and Xu, R. M. (2006) Recognition of histone H3 lysine-4 methylation by the double Tudor domain of JMJD2A. *Science* **312,** 748–751
58. Corsini, L., and Sattler, M. (2007) Tudor hooks up with DNA repair. *Nat. Struct. Mol. Biol.* **14,** 98–99
59. Friberg, A., Oddone, A., Klymenko, T., Müller, J., and Sattler, M. (2010) Structure of an atypical Tudor domain in the *Drosophila* Polycomb-like protein. *Protein Sci.* **19,** 1906–1916
60. Bienz, M. (2006) The PHD finger, a nuclear protein-interaction domain. *Trends Biochem. Sci* **31,** 35–40
61. Mellor, J. (2006) It takes a PHD to read the histone code. *Cell* **126,** 22–24
62. Bracken, A. P., and Helin, K. (2009) Polycomb group proteins. Navigators of lineage pathways led astray in cancer. *Nat. Rev. Cancer* **9,** 773–784
63. Schuettengruber, B., and Cavalli, G. (2009) Recruitment of Polycomb group complexes and their role in the dynamic regulation of cell fate choice. *Development* **136,** 3531–3542
64. Sing, A., Pannell, D., Karaiskakis, A., Sturgeon, K., Djabali, M., Ellis, J., Lipshitz, H. D., and Cordes, S. P. (2009) A vertebrate Polycomb response element governs segmentation of the posterior hindbrain. *Cell* **138,** 885–897
65. Woo, C. J., Kharchenko, P. V., Daheron, L., Park, P. J., and Kingston, R. E. (2010) A region of the human HOXD cluster that confers Polycomb-group responsiveness. *Cell* **140,** 99–110
66. Villa, R., Pasini, D., Gutierrez, A., Morey, L., Occhionorelli, M., Viré, E., Nomdedeu, J. F., Jenuwein, T., Pelicci, P. G., Minucci, S., Fuks, F., Helin, K., and Di Croce, L. (2007) Role of the Polycomb repressive complex 2 in acute promyelocytic leukemia. *Cancer Cell* **11,** 513–525
67. Herranz, N., Pasini, D., Díaz, V. M., Francí, C., Gutierrez, A., Dave, N., Escrivà, M., Hernandez-Muñoz, I., Di Croce, L., Helin, K., García de Herreros, A., and Peiró, S. (2008) Polycomb complex 2 is required for E-cadherin repression by the Snail1 transcription factor. *Mol. Cell. Biol.* **28,** 4772–4781
68. Hansen, K. H., Bracken, A. P., Pasini, D., Dietrich, N., Gehani, S. S., Monrad, A., Rappsilber, J., Lerdrup, M., and Helin, K. (2008) A model for transmission of the H3K27me3 epigenetic mark. *Nat. Cell Biol.* **10,** 1291–1300
69. Pasini, D., Bracken, A. P., Hansen, J. B., Capillo, M., and Helin, K. (2007) The Polycomb group protein Suz12 is required for embryonic stem cell differentiation. *Mol. Cell. Biol.* **27,** 3769–3779
70. Rood, B. R., Zhang, H., Weitman, D. M., and Cogen, P. H. (2002) Hypermethylation of HIC-1 and 17p allelic loss in medulloblastoma. *Cancer Res.* **62,** 3794–3797
71. Boldajipour, B., Mahabaleshwar, H., Kardash, E., Reichman-Fried, M., Blaser, H., Minina, S., Wilson, D., Xu, Q., and Raz, E. (2008) Control of chemokine-guided cell migration by ligand sequestration. *Cell* **132,** 463–473
72. Sierro, F., Biben, C., Martínez-Muñoz, L., Mellado, M., Ransohoff, R. M., Li, M., Woehl, B., Leung, H., Groom, J., Batten, M., Harvey, R. P., Martínez-A, C., Mackay, C. R., and Mackay, F. (2007) Disrupted cardiac development but normal hematopoiesis in mice deficient in the second CXCL12/SDF-1 receptor, CXCR7. *Proc. Natl. Acad. Sci. U.S.A.* **104,** 14759–14764
73. Dodelet, V. C., and Pasquale, E. B. (2000) Eph receptors and ephrin ligands. Embryogenesis to tumorigenesis. *Oncogene* **19,** 5614–5619